



Development, scrutiny, and modulation of transient reporter gene assays of the xenobiotic metabolism pathway in zebrafish hepatocytes

Sebastian Lungu-Mitea · Yuxin Han ·
Johan Lundqvist

Received: 7 March 2021 / Accepted: 25 September 2021 / Published online: 15 October 2021
© The Author(s) 2021

Abstract The “toxicology in the twenty-first century” paradigm shift demands the development of alternative in vitro test systems. Especially in the field of ecotoxicology, coverage of aquatic species-specific assays is relatively scarce. Transient reporter gene assays could be a quick, economical, and reliable bridging technology. However, the user should be aware of potential pitfalls that are influenced by reporter vector geometry. Here, we report the development of an AhR-responsive transient reporter-gene assay in the permanent zebrafish hepatocytes cell line (ZFL). Additionally, we disclose how viral, constitutive promoters within reporter-gene assay cassettes induce squelching of the primary signal. To counter this, we designed a novel normalization vector, bearing an endogenous zebrafish-derived genomic promoter (zfEF1aPro), which rescues the squelching-delimited system, thus, giving new insights into the modulation of transient reporter systems under xenobiotic stress. Finally, we uncovered how the ubiquitously used ligand BNF promiscuously activates multiple toxicity pathways of the xenobiotic metabolism

and cellular stress response in an orchestral manner, presumably leading to a concentration-related inhibition of the AhR/ARNT/XRE-toxicity pathway and non-monotonous concentration–response curves. We named such a multi-level inhibitory mechanism that might mask effects as “maisonette squelching.”

Keywords Bioassays · Reporter gene assays · Transient transfection · Fish cell lines · Squelching

Introduction

Within the last two decades, several chemical regulation bills (The European Parliament and the Council 2003, 2006, 2009; US EPA 2016) were conceptualized, ratified, and utilized on an international level, intending the proper protection of humankind and the surrounding environment from anthropogenically derived compounds. Unfortunately, increasing demands in toxicological in vivo testing triggered the dilemma of weighing risk assessment against economic feasibility and ethical standards (Goldberg 2010; Hartung 2010, 2011). This development contradicts efforts made within the scientific community to promote the acceptance and use of the “3Rs” (Russell and Burch 1959; Lillicrap et al. 2016). The use of alternative or new approach methods (NAMs), such as in vitro and in silico based applications, for the detection and measurement of “toxicity pathways” (TPs), has been postulated as a primary concept of

Supplementary Information The online version contains supplementary material available at <https://doi.org/10.1007/s10565-021-09659-0>.

S. Lungu-Mitea (✉) · Y. Han · J. Lundqvist
Department of Biomedicine and Veterinary Public Health,
Swedish University of Agricultural Sciences, Box 7028,
750 07 Uppsala, Sweden
e-mail: sebastian.lungu@slu.se

the “toxicology in the twenty-first century” (Tox21) framework (NRC 2007; Collins et al. 2008; Whelan and Andersen 2013; Kleensang 2014). A TP is defined as a sequence of intracellular events, which maintain cellular homeostasis under physiological conditions, but once perturbed by a xenobiotic, may lead to adverse effects on the cellular and, beyond, on the organismal level of biological complexity (Whelan and Andersen 2013). Shortly after, TPs were augmented by the adverse outcome pathway (AOP) concept (Ankley et al. 2010), which projects the TP concept onto the population and community scale and adds elements of network plasticity.

TPs of the xenobiotic metabolism are among the best studied. Ligand-dependent recruitment of the aryl hydrocarbon receptor (AhR) transcription factor by xenobiotics, the translocation sequestered by its dimerization partner the aryl hydrocarbon receptor nuclear translocator (ARNT), binding to the xenobiotic response element (XRE), and synthesis of downstream phase I and II xenobiotic metabolism enzymes have extensively been researched and are well-documented in the literature (reviewed in Schmidt and Bradfield 1996)). The AhR is known to be promiscuous. Firstly, in the sense that it binds exogenous and endogenous ligands with different affinities (Soshilov and Denison 2014; Tagliabue et al. 2019), and secondly, in terms of downstream activation and cross-talk with non-canonical pathways by dimerization with alternate translocators and transcriptional cofactors (reviewed in Denison and Faber 2017)).

Reporter gene assays are an ubiquitous tool for screening TPs (Zacharewski 1997; Ankley et al. 1998; Mueller 2004; Leusch and Snyder 2015), given their intrinsic ability to define molecular initiating events (MIE) and mechanism of action (MOA). Reporter gene assays comprise pro and eukaryotic cellular systems bearing stably or transiently introduced reporter gene cassettes. The cassettes are composed of a specific genomic or synthetic TP-related response element, fused to a reporter enzyme coding sequence, such as luciferase or the green fluorescence protein. Upon activation of the TP-specific response element, the utilized reporter is synthesized in parallel to the TP-specific target genes and enzymes. The reporter signal is quantifiable, thus disclosing the turnover of the TP-specific target genes to the investigator. Some reporter gene and catalytic enzyme assays for assessing xenobiotic metabolism-related toxicity have

been established, mainly in rodent cell lines, and proved successful in various fields of toxicity testing (reviewed in Eichbaum et al. 2014)).

However, within ecotoxicology, coverage of TPs by species-specific reporter assays is relatively scarce, and a couple of strategy papers encouraged their development within the last years (EURL-ECVAM 2014; Halder et al. 2014; Worth et al. 2014). Nonetheless, the AhR/ARNT/XRE TP is the best established in terms of available assays, especially in comparison to other TPs. A few reporter gene assays have been developed in rainbow trout (*Oncorhynchus mykiss*) (Richter et al. 1997; Villeneuve et al. 1999) and zebrafish (*Danio rerio*) cell lines (Carvan et al. 2000; Mattingly et al. 2001; Yang et al. 2016; Chen and Chan 2017; Zhou et al. 2017). The zebrafish offers a toxicity testing platform of great potential. The fish embryo test (FET) was one of the first in vitro assays to gain partly regulatory acceptance (OECD 2013; Belanger et al. 2013). Further, the zebrafish is a standard test species in developmental molecular biology, and a plethora of biotechnological tools is available. Thus, a few transgenic zebrafish strains have already been established and can be used in parallel to cellular assays to identify and measure TPs, also facilitating in vitro to in vivo extrapolation (IVIVE) studies (reviewed in Garcia et al. 2016)). Beyond, all AhR/ARNT/XRE pathway components were successfully characterized in zebrafish (Tanguay et al. 1999, 2000; Andreassen et al. 2002; Zeruth and Pollenz 2005, 2007; Hahn et al. 2017), hence, enabling the investigator to draw mechanistic conclusions. The demand for reliable reporter gene assays indicating critical toxicity endpoints within ecotoxicology is on the rise, given the fact that the current European Water Framework Directive (WFD) is approaching its deadline in 2027. A potential continuation of the directive will propose the addition of effect-based and directed tools (bioassays) to accompany classical chemical analysis in environmental screenings (Wernersson et al. 2015; Brack et al. 2017, 2018, 2019). The discussion has yet been indecisive regarding to what amount established mammalian assays should be incorporated or if assays derived from aquatic organisms are more representative (Lillicrap et al. 2016; Neale et al. 2020).

In comparison to stably transfected constructs, transient reporter gene assays have the advantage of being more flexible and more comfortable to handle regarding logistics and maintenance. One primary permanent

cell line can be used and transiently transfected with different constructs, thus covering the assessment of various TPs. Further, the distribution of reporter-containing plasmid DNA is more straightforward than the distribution of living cells. Finally, reporter constructs on plasmid DNA are easily accessible and can be modified by the investigator to fit their specific needs. However, there might be a misconception regarding reporter gene assays' overall reliability and correct application. Notably, stable or transient transgenesis of non-endogenous genetic constructs will interfere with the host organism on genomic, epigenetic, and phenotypic levels. Thus, the manipulated model system might be impacted beyond the inquired pathway's response and produce nonspecific results (reviewed in Stepanenko and Heng 2017). Recently, we assessed the issue of transient transgenesis in zebrafish cell lines, displaying significant differences in reporter gene assay potency, efficacy, and reliability in regard to plasmid vector geometry (Lungu-Mitea and Lundqvist 2020). Transient transfection is impacted synergistically in terms of vector sizes, vector backbones, gene-regulatory units, tissue origin, transfection method, and dual luciferase signal normalization. Further, we proposed strategies to account for spurious TP regulation and how to approach the design of transient TP-related reporter gene assays.

This study aimed to design a potent transient reporter gene assay of the AhR-related xenobiotic metabolism TP in the permanent zebrafish hepatocyte cell line (ZFL) (Ghosh et al. 1994). In the perspective of our previous work, we wanted to examine spurious up or down-regulation of the TP-mediated signal in transiently transfected cells under stress by chemical exposure. Thus, we hypothesized that the potency and efficacy of a compound, as recorded by the reporter gene assay, might be affected by the vector geometry, most likely by the inherent gene-regulatory units. Additionally, we hypothesized to encounter synergistically acting cellular stress due to synchrony of transfection and exposure, which might alternate the recoded signal in a specific way.

Materials and methods

Chemicals

Known AhR-agonists β -naphthoflavone (BNF; $\geq 98\%$ purity; Sigma-Aldrich, Steinheim, Germany) and

2,3,7,8-tetrachlorodibenzo-p-dioxin (TCDD; 10 $\mu\text{g}/\text{mL}$ in toluene; Supelco analytical standard; Sigma-Aldrich, Steinheim, Germany) were used in all experiments. BNF powder was dissolved in dimethyl sulfoxide (DMSO; anhydrous, $\geq 99.9\%$ purity, sterile; Sigma-Aldrich, Steinheim, Germany) to a 20-mM stock concentration. The toluene solvent in the TCDD vial was evaporated, and crystalized TCDD redissolved in DMSO to a 32- μM stock concentration. Both BNF and TCDD stock solutions were aliquoted into minor volumes to thaw only one vial per week/experiment. Stocks were stored at $-20\text{ }^{\circ}\text{C}$ in a desiccator.

Cell culturing

The zebrafish liver cell line (CVCL_3276) (Ghosh et al. 1994) was purchased from ATCC (Mannassas, USA). A nutrition medium consisting of 50% (v/v) Leibovitz's L-15 (Sigma-Aldrich, Steinheim, Germany), 35% (v/v) Dulbecco's modified Eagle's medium (Gibco, Paisley, UK), 15% (v/v) Ham's Nutrient Mixture F-12 (Gibco, Paisley, UK), and phenol red, supplemented by 150 mg/L sodium bicarbonate (Gibco, Paisley, UK), 15 mM HEPES (Gibco, Paisley, UK), 10 $\mu\text{g}/\text{mL}$ bovine insulin (Sigma-Aldrich, Steinheim, Germany), 50 ng/mL mouse EGF (Sigma-Aldrich, Steinheim, Germany), and 5% (v/v) fetal bovine serum (Gibco, Paisley, UK), was used for cultivation. The cells were cultured in a humidified environment at $28\text{ }^{\circ}\text{C}$ and atmospheric CO_2 . Further, cells were passaged weekly in a 1:20 subcultivation ratio. Phosphate buffered saline (PBS, pH 7.4; Medicago, Uppsala, Sweden) was used for washing and 0.25% (w/v) trypsin-EDTA (Sigma-Aldrich, Steinheim, Germany) for cell detachment. All experiments were conducted within passage numbers 5 to 32.

Plasmids and cloning

The **pGL4.43[luc2p/XRE/hygro]** plasmid was acquired from Promega (Madison, USA). The latter consists of a pGL4 backbone including an ampicillin resistance gene, a gene for hygromycin resistance, and three copies of a synthetic xenobiotic response element (XRE) driving transcription of the Firefly luciferase reporter gene luc2P (*Photinus*

pyralis). The **pGudLuc7.5** plasmid was donated by Michael S. Denison (University of California, Davies, USA). The latter consists of a **pGL3** backbone, 20 XRE copies from the genomic promoter region of the *mCyp1A1* gene upstream of an MMTV viral promoter, and the Firefly luciferase reporter gene (Denison et al. 1989; El-Fouly et al. 1994; Garrison et al. 1996; Han et al. 2004; He et al. 2011). Firefly luciferase was used as the primary reporter in this study.

Plasmids of the **pRL** and **pGL4** series were also acquired from Promega. All plasmids consist of a **pRL** or **pGL4** backbone including the cDNA encoding for Renilla luciferase reporter gene (*Renilla reniformis*) and a specific constitutive promoter sequence of viral origin (Table 1, Fig. S2): **pRL-null/ pGL4.70**: minimal promoter (minP); **pRL-SV40/ pGL4.73**: simian virus 40 promoter; **pRL-TK/ pGL4.74**: herpes simplex virus thymidine kinase promoter; **pRL-CMV/ pGL4.75**: cytomegalovirus promoter. Renilla luciferases were used as control/normalization signals in the following dual reporter gene assays (DLR).

The “**ZF-L Exp**” plasmid, containing the zebrafish translation elongation factor 1 alpha promoter (*zEF1aPro*), was donated by Patrick Heinrich (University of Heidelberg, Germany) (Heinrich and Braunbeck 2018). *zEF1aPro* cDNA was initially amplified from an adult female Westaquarium strain zebrafish and cloned into the “**ZF-L Exp**” vector. Within the “**ZF-L Exp**” vector, the *zEF1aPro* fragment (1.4 kB) is flanked by a *Bgl*III and an *Xho*I restriction site at the respective 5' and 3' ends, which allows easy insertion into the multiple cloning site

(MCS) of the pRL-null plasmid in the forward direction. Restriction digestion, ligation, and propagation of the newly designed plasmid **pRL-null[zEF1aPro]** (Fig. S1) are described in detail in the supplementary information (SI).

ZFL cells were also transiently co-transfected with the **pGL4.37** and **pRL-CMV** vector pair to study potential impacts on the oxidative stress response pathway after BNF exposure. A transient reporter gene assay for the assessment of oxidative stress in the ZFL cell line had been described previously (Lungu-Mitea and Lundqvist 2020), and was applied here in an identical manner. Please consult the respective chapter within the SI for more details.

Handling, transient transfection, and exposure

ZFL cells were seeded either into white, clear-bottom 96-well microtiter plates (Corning, New York, USA; for DLR assays) or transparent 96-well microtiter plates (Corning, New York, USA; for viability assays) at a density of 1.5×10^5 cells/mL, in 100 μ L/well. After 24 h of incubation, cells reached a confluence of about 80%.

The transient transfection was conducted in a 2- μ g transfection reagent to 1 μ g plasmid DNA ratio, applying the XHP transfection reagent (Roche, Mannheim, Germany). Specific transfection optimization experiments were reported priority (Lungu-Mitea et al. 2018). The transient transfection reaction was incubated as a co-transfection in a 10:1 reporter to control ratio (0.9 μ g reporter plasmid, 0.1 μ g control plasmid) for 30 min, before adding the reaction mixture to the cells. Firefly luciferase-bearing vectors were used as the primary

Table 1 Used plasmid vectors, their specific promoter (+enhancer in some cases), and the luciferase reporter. Consult Figs. S1 and S2 for the plasmid vector geometry

Plasmid vector	Promoter/enhancer	Reporter	Size [nt]
pGL4.43[luc2p/XRE/hygro]	3 × XRE (synthetic) + minP	Firefly	6067
pGudLuc7.5	20 × XRE (genomic) + MMTV	Firefly	~ 8300
pGL4.70[hRluc]	minP	Renilla	3522
pGL4.73[hRluc/SV40]	SV40	Renilla	3921
pGL4.74[hRluc/TK]	TK	Renilla	4237
pGL4.75[hRluc/CMV]	CMV	Renilla	4281
pRL-null	minP	Renilla	3320
pRL-SV40	SV40	Renilla	3705
pRL-TK	TK	Renilla	4045
pRL-CMV	CMV	Renilla	4079
pRL-null[zEF1aPro]	zEF1aPro + minP	Renilla	4795

reporter plasmids, and Renilla luciferase-bearing vectors were used for normalization (control plasmid). Ten microliter per well of the transfection reaction mix was added to the cells and incubated for 24 h. Following (Lungu-Mitea and Lundqvist 2020), cells used in both DLR and viability assays were transiently transfected.

After 24 h of post-transfection incubation, cells were exposed to known AhR-agonists BNF or TCDD. Prepared aliquots of stock solutions were thawed and further titrated using the nutrition medium supplemented with 5% (v/v) DMSO as a solvent. Seeded cells on 96-well plates were exposed in triplicates to increasing nominal concentrations of BNF and TCDD. Different exposure regimes were applied. In terms of BNF, cells were first exposed to concentrations of 3, 30, and 300 nM. All potential co-transfection combinations were screened in this initial approach. Candidate plasmids that scored higher overall induction values were reassessed in an exposure regime of 300 pM to 1 μ M BNF (0.3, 1, 3, 10, 30, 100, 300, 1000 nM). Further, cells transfected with candidate plasmid combinations were subjected to a TCDD exposure regime from 100 pM to 100 nM (0.1, 0.3, 1, 3, 10, 30, 100 nM). Cells were exposed in 100 μ L/well of the specifically spiked nutrition medium. Solvent controls (negative controls) were conducted in six replicates for every specific experiment.

Dual reporter gene assay

After 24 h of exposure to AhR-agonists, cells on white 96-well microtiter plates were lysed in 20- μ L passive lysis buffer (PLB; Promega, Madison, USA), and quantitative AhR-dependent luminescence was measured via Dual-Luciferase® Reporter Assay (DLR; Promega, Madison, USA), according to the manufacturer's protocol using an auto-injecting Infinite M1000 microplate reader (Tecan, Männedorf, Switzerland), following a flash luminescence protocol. The luciferase activity was normalized to transfection efficiency (Firefly raw light unit readout divided by Renilla raw light unit readout) and further expressed as fold change compared to the non-treated controls.

Viability testing

In parallel to the DLR assays, MTS/BCA-multiplex assays were conducted on identically treated cells.

The MTS/BCA-multiplex assay, which is described in detail in (Lungu-Mitea et al. 2021), scores NADPH-turnover and total protein amount as apical endpoints of cell viability or cytotoxicity. After 24 h exposure, the spiked nutrition medium was discharged, cells were washed once in 100 μ L/well PBS, and 100 μ L/well Earle's Balanced Salt Solution (EBSS; Gibco, Paisley, UK) was added. MTS-based CellTiter 96® Aqueous One Solution Cell Proliferation Assay (Promega, Madison, USA) was conducted following the manufacturer's protocol. Seventeen percent (v/v) MTS reagent were added to the wells. After 2 h of incubation at 28 °C and atmospherical CO₂, formazan product turnover absorbance was measured at 490 nm using an Infinite M1000 microplate reader. Afterwards, EBSS and MTS reagents were removed. Cells were washed once in 100 μ L/well PBS and lysed in 20- μ L PLB at RT for 30 min. Bicinchoninic Acid Protein Assay (BCA, Sigma-Aldrich, St. Louis, USA) was conducted following the manufacturer's protocol. One hundred eighty microliters of BCA-reagent was added to every well, plates were agitated shortly, and incubated for 20 min at 60 °C. After cooling down for 15 min at RT, absorbance was measured at 562 nm using an Infinite M1000 microplate reader.

Statistical analyses

Data of the DLR and the multiplex viability assays were processed and illustrated in GraphPad Prism 8 (GraphPad Software, La Jolla, USA). Study design to determine EC_x concentrations was conducted according to guidelines and recommendations (Green et al. 2018; Musset 2018), with at least six exposure concentrations in triplicates. However, initial screening experiments with BNF were conducted as a NOEC/LOEC analysis.

In terms of the NOEC/LOEC analyses, for both approaches (DLR and viability), mean background values (blanks) were subtracted from the raw values, and the data was computed as fold induction in relation to the negative controls. Means of every experiment were pooled (experimental unit n=3–5; observational unit N=9–15). Normality was tested by Shapiro–Wilk and Kolmogorov–Smirnov tests (both significance level alpha=0.05) and analyzed graphically via normal-qq-plot. Non-normal data were log-transformed and re-analyzed. Given normality, statistically differing significance in the output signal

from the negative controls was assessed via one-way ANOVA, followed by Dunnett's post hoc test (for multiple comparisons vs. control). Residuals were graphically analyzed by quantile–quantile plot (actual vs. predicted residuals), homoscedasticity plot (absolute residuals vs. fitted), and residual plot (residuals vs. fitted) to ensure ANOVA criteria were met. Further, Brown–Forsythe and Bartlett's tests were conducted to check for the residuals' homoscedasticity and normality. Beyond statistical significance, for all viability tests, a threshold of 80% as compared to the negative control (corresponding 0.8) was determined as biologically significant and marked with a dotted red line within all respective graphs.

In terms of the EC_x (effect concentrations) and IC_x (inhibitory concentrations) regression analyses, DLR data was either assessed as relative induction or normalized induction (100 = max. overall fold response; 0 = min. overall fold response), given that normalized data results in overall better regression fits but is unable to display differences in efficacy. For EC_{50} and EC_{20} estimation, data were fitted to a four-parameter log-logistic (4PL) model with alternations described by (Weimer et al. 2012). Hence, curves were not fitted to upper and lower boundaries, but the controls were included in the regression as anchor values. Non-monotonous concentration–response curves (NMCRs) were fitted likewise, using a bell-shaped nonlinear regression (as documented in https://www.graphpad.com/guides/prism/8/curve-fitting/reg_bells_haped_dose_response.htm).

Overall effects of the transfection setup on the recorded signal were analyzed via two-way ANOVA followed by Tukey's post hoc test for multiple comparisons, with exposure concentrations and transfection setups both used as factors. An assessment of residuals was conducted, as stated above.

Results

Screening experiments of co-transfected normalization vectors

In accordance with a previous study (Lungu-Mitea and Lundqvist 2020), both primary Firefly luciferase bearing reporter vectors were tested in transient co-transfection with all acquired normalization vectors. The normalization vectors were of two variations,

consisting of either a **pGL4** or **pRL** backbone (Table 1, Fig. S2). Additionally, transcription of the Renilla luciferase normalization signal was either sequestered by a viral promoter (SV40, TK, CMV) or a minimal promoter construct (minP) on the respective backbone. Hence, eight normalization vectors were tested in the initial screening experiments. For the reporter vectors, two different constructs were tested. **pGL4.43** bears a synthetic promoter consisting of three repeat copies of the XRE core consensus sequence, fused to minP. **pGudLuc7.5** carries a genomic promoter of the *mCYP1A1* gene consisting of twenty copies of the mouse XRE sequence linked to the MMTV promoter (Han et al. 2004; He et al. 2011). Accordingly, a total of sixteen experimental setups was conducted within the first screening phase (Figs. 1, 2, S3, and S4). Cells transiently co-transfected with the specific setups were exposed to three increasing concentrations of BNF. Promising co-transfection setups were further tested in an entire concentration–response exposure regime (300 pM to 1 μ M) (Figs. 1, 3, and S5). BNF was initially chosen as an agonist in the screening experiments due to less complicated handling and lower occupational hazard. Cellular viability was tested in parallel on identically co-transfected cells via the MTS/BCA-multiplex assay.

Appropriate AhR-related signal induction was only recorded for the **pGL4.43** reporter in combination with both normalization vectors that did not bear any viral promoters (Figs. 1A + B and 2). For the **pGL4.43 + pGL4.70** combination (Fig. 1A), the LOEC and the highest fold-induction of 4.1 were recorded at 10 nM. For the **pGL4.43 + pRL-null** combination (Fig. 1B), the LOEC and highest fold-induction of 3.9 was also recorded at 10 nM. Interestingly, BNF exposure did not induce an increasing or sigmoidal concentration–response curve. Instead, after AhR-related signal activation is peaking at around 10–30 nM, signal inhibition is encountered beyond 30 nM of BNF. The highest exposure concentration of 1 μ M BNF led to statistically significant inhibition of the AhR-related signal in both co-transfection combinations. However, no statistically significant cytotoxicity was recorded for any of the apical endpoints tested within the entire concentration range (Fig. 1). Arguably, a slight trend in decline was detectable for the MTS endpoint beyond 300 nM BNF (Fig. 1A + B). Co-transfection with **pGudLuc7.5**

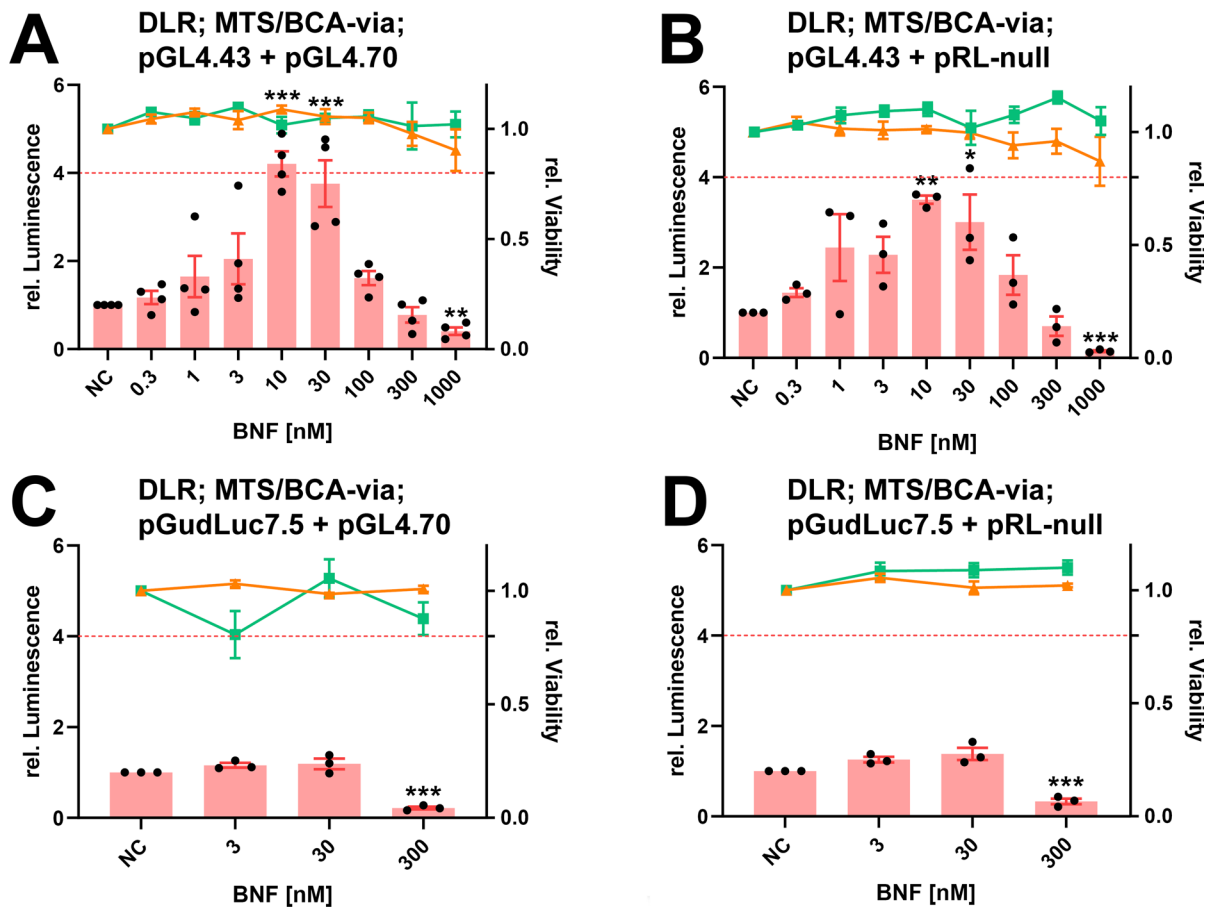


Fig. 1 Effects on luminescence measured in the zebrafish cell line ZFL exposed to BNF. Luminescence corresponds to quantitative AhR transcription factor activation, measured via DLR assay in cells co-transfected with the depicted combinations of reporter and normalization vectors (A–D; all non-viral promoters). Mean normalized luminescence induction is illustrated as red bars, black dots represent means of single experiments, and red whiskers represent the SEM (experimental units $n=3-4$;

observational units $N=9-12$). Cellular viability corresponds to apical endpoints measured via the MTS/BCA-multiplex assay. Each point (MTS orange, BCA green) represents the mean, including SEM (experimental units $n=3-4$; observational units $N=9-12$). A threshold value of 0.8 was considered biologically significant (dotted red line). Asterisks indicate significance tested in a one-way ANOVA with Dunnett's post hoc test (* $P < 0.05$, ** $P < 0.01$, *** $P < 0.001$)

resulted in no overall statistically significant induction of the AhR-related luciferase signal (Figs. 1C+D, 2, and S4). Nevertheless, the 300 nM BNF exposure concentration caused a statistically significant inhibition of the AhR-related signal for the non-viral promoter combinations (Fig. 1C+D) as well. Once more, no statistical significant cytotoxicity was recorded.

The pGL4.43 vector also showed statistically significant induction in co-transfection with normalization vectors bearing viral promoters (Figs. 2 and S3). Statistically significant induction of the AhR-related luciferase response was recorded for the

co-transfection combination pGL4.43 + pGL4.74 (Fig. S3A), pGL4.43 + pRL-SV40 (Fig. S3D), and pGL4.43 + pGL4.73 (Fig. S3C). However, the induction was only within a 1.5- to threefold scale. Plasmids bearing TK-promoters also showed a downregulation of the signal in the highest exposure concentration (Fig. S3A+B). No statistically significant cytotoxicity was recorded for pGL4.43 in combination with any viral promoter-bearing vector. However, pRL-SV40 and pRL-CMV depicted cytotoxicity by biological threshold definition within the highest exposure concentration for at least one endpoint of cytotoxicity (Fig. S3D+F). The pGudLuc7.5 vector showed

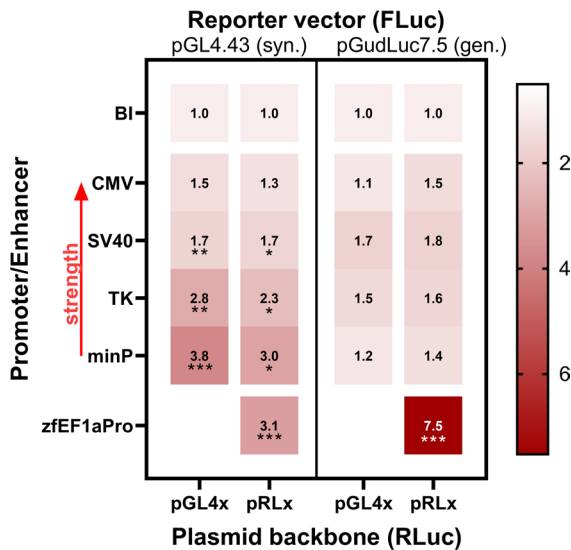


Fig. 2 A heatmap summarizing AhR-activation related fold induction of all screening experiments at a 30-nM BNF exposure concentration. A total of 16 experimental transient co-transfection combinations has been conducted. The primary Firefly luciferase (FLuc) reporter vectors pGL4.43 (synthetic response element) and pGudLuc7.5 (genomic response element) were co-transfected with 8 Renilla luciferase (RLuc) normalization vectors of the pGL4 and pRL backbone series. The normalization vectors are bearing constitutive promoters of increasing strength (CMV > SV40 > TK > minP; red arrow), driving background RLuc expression. Maximum relative fold induction is given in relation to negative controls (base level induction, BI). Numerical fold induction is given for every combination. Transient co-transfection results are given for the respective pRL-null[zfEF1aPro] combinations, as well. Asterisks indicate significance tested in a one-way ANOVA with Dunnett's post hoc test (vs. control BI; * P < 0.05, ** P < 0.01, *** P < 0.001)

no significant statistical induction for any viral promoter-bearing normalization vectors in co-transfection (Figs. 2 and S4). Tentatively, an inhibition is detectable for TK and SV40-bearing vectors within the highest exposure concentrations (Fig. S4A-D). Cytotoxicity was recorded for CMV and SV40-bearing vectors within the highest exposure concentration, at least within one apical endpoint, in terms of either statistical or biological significance (Fig. S4C-F).

The endogenous zfEF1a promoter restores AhR-related luciferase induction after BNF exposure

Given that only normalization vectors without viral promoters resulted in an appropriate signal induction,

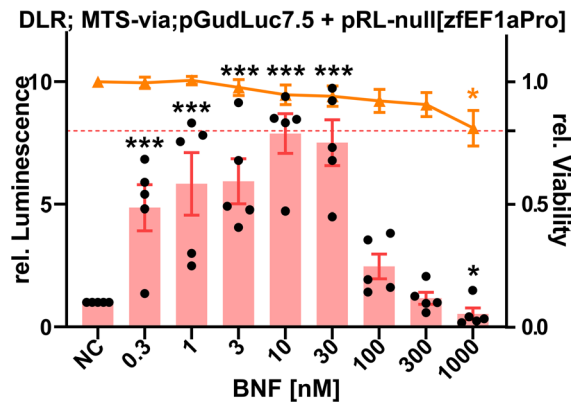


Fig. 3 Effects on luminescence measured in the zebrafish cell line ZFL exposed to BNF. Luminescence corresponds to quantitative AhR transcription factor activation measured via DLR assay in cells co-transfected with the pGudLuc7.5 reporter and pRL-null[zfEF1aPro] normalization vector. Mean normalized luminescence induction is illustrated as red bars, black dots represent means of single experiments, and red whiskers represent the SEM (experimental units $n=5$; observational units $N=15$). Cellular viability corresponds to formazan turnover in the MTS viability assay. Each orange point represents the mean, including SEM (experimental units $n=5$; observational units $N=15$). A threshold value of 0.8 was considered biologically significant (dotted red line). Asterisks indicate significance tested in a one-way ANOVA with Dunnett's post hoc test (* P < 0.05, ** P < 0.01, *** P < 0.001)

pRL-null was chosen as a template for directional cloning of the endogenous zebrafish translation elongation factor 1 alpha genomic promoter (zfEF1aPro). The pRL-null multiple cloning site (MCS) exhibited a priori the correct topography to insert zfEF1aPro in the forward direction, whereas pGL4.70 would have required additional assembly PCRs. Subsequently, the newly cloned pRL-null[zfEF1aPro] normalization vector (Fig. S1) was co-transfected with both used reporter vectors. The pGL4.43 + pRL-null[zfEF1aPro] co-transfection was almost identical to pGL4.43 + pRL-null, with the former depicting a slightly lower LOEC (3 nM) and an identical maximum induction of 3.9-fold at a concentration of 10 nM (Fig. S5). However, increased LOEC sensitivity might derive from the higher amount of replicates used in the statistical test ($n=5$ vs. $n=3$). Nevertheless, the pGudLuc7.5 + pRL-null[zfEF1aPro] co-transfection setup showed significant differences from the pGudLuc7.5 + pRL-null setup. Integration of the genomic zfEF1a promoter restored the BNF-induced luminescence signal (Figs. 2 and 3). Maximal

induction almost doubled to 7.9-fold (10 nM BNF), and the LOEC was reduced to 300 pM. Arguably, a more sensitive LOEC could have been measured if the exposure regime were accordingly adapted. In accordance with the screening experiments, concentrations beyond 30 nM BNF induced inhibition of the AhR-related luminescence signal. Statistically significant cytotoxicity was recorded at a concentration of 1 μM BNF. Here, only the MTS endpoint was measured since the screening experiments depicted no systemic difference between the MTS and BCA endpoints.

The data of the most advantageous co-transfection setups were additionally fitted to bell-shaped concentration–response nonlinear regressions, with alternations according to (Weimer et al. 2012) (Fig. 4). EC₅₀ (50% effective concentration), IC₅₀ (50% inhibitory concentration), and PC_{max} (maximum peak concentrations)

were respectively derived from the regressions (Table 2). The nonlinear regressions were either computed with the relative induction data (Fig. 4A), as also depicted in the previous graphs (Figs. 1 and 3), or with normalized induction data (0–100% response, Fig. 4B). Normalized data often results in better fits (see parameters of fit, adjusted R² and NRSME values in Table 2) but is not suited for displaying differences in efficacy. Overall, the **pGudLuc7.5 + pRL-null[zfEF1aPro]** co-transfection setup depicted the highest efficacy with the relative induction of the luciferase signal plateauing at 7.9-fold (Fig. 4A). At the same time, the **pGL4.43 + pGL4.70** and **pGL4.43 + pRL-null** co-transfection setups showed similar plateaus in the 3.5 to 4.2-fold induction range. Interestingly, the **pGudLuc7.5 + pRL-null[zfEF1aPro]** (EC₅₀ 63 pM) and **pGudLuc7.5 + pRL-null** (EC₅₀ 490 pM) setups depicted gentler slopes than **pGL4.43 + pGL4.70**

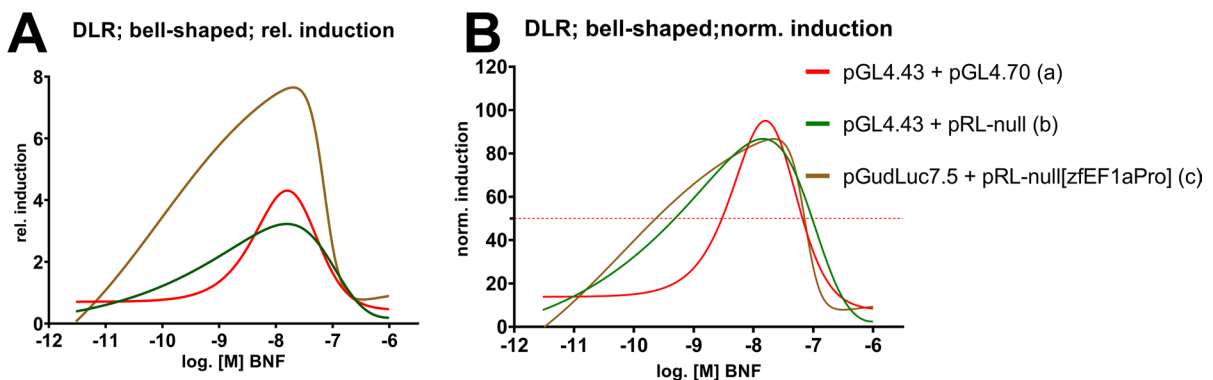


Fig. 4 Bell-shaped concentration–response curves of depicted co-transfection setups after BNF exposure. Results of the DLR assays were either fitted as relative induction (A) or normal-

ized induction values (B) to the nonlinear regression. EC₅₀, IC₅₀, and PC_{max} values are summarized in Table 2. Specific concentration–response curves are illustrated in Fig. S6

Table 2 LOEC, EC₅₀/IC₅₀, and PC_{max} values derived from BNF exposure (adj. R² and NRSME values are given as goodness-of-fit parameters of the nonlinear regression)

Transfection setup (according to Fig. 4)	LOEC (adj. P-value)	EC ₅₀ (normalized; adj. R ² ; NRSME)	IC ₅₀ (normalized; adj. R ² ; NRSME)	EC ₅₀ (relative; non-normalized; adj. R ² ; NRSME)	IC ₅₀ (relative; non-normalized; adj. R ² ; NRSME)	PC _{max} (relative, non-normalized)	N (exp.)
(a) pGL4.43 + pGL4.70	10 nM (<0.0001)	2.95 nM (0.8; 0.39)	24 nM (0.80; 0.32)	2.45 nM (0.77; 0.02)	27 nM (0.77; 0.02)	15.8 nM (0.77; 0.02)	4
(b) pGL4.43 + pRL-null	10 nM (0.0044)	490 pM (0.71; 0.71)	106 nM (0.72; 0.55)	309 pM (0.72; 0.03)	109 nM (0.72; 0.02)	15.7 nM (0.72; 0.02)	3
(c) pGudLuc7.5 + pRL-null[zfEFaprop]	300 pM (0.003)	63 pM (0.79; 0.31)	73 nM (0.79; 0.31)	87 pM (0.75; 0.03)	72 nM (0.75; 0.03)	19.5 nM (0.75; 0.03)	5

(EC_{50} 3 nM), thus also showing an increased potency to the BNF exposure. PC_{max} were per se similar, ranging from 15.7 to 19.5 nM, indicating a common peak concentration, regardless of the co-transfection setup. The IC_{50} values were all in the same range, approximately 20–100 nM, regarding the regression model used. Hence, the inhibition in higher BNF concentrations is not affected by the co-transfection setup used but derives from another common systemic mechanism. Comparison of overall mean co-transfection setup effects resulted in no statistical differences for the normalized data. Still, the **pGudLuc7.5 + pRL-null[zfEF1aPro]** combination is statistically differing from the other two in terms of relative induction

Table 3 Comparison of mean co-transfection setup effects between combinations depicted in Fig. 4 and Table 2. Statistical significance in mean setup effect was assessed via 2-way ANOVA, followed by Tukey's post hoc test (ns $P > 0.05$, *** $P < 0.001$)

Comparison	Adjusted P -value	Significance
a vs. b (rel.; Fig. 4A)	0.8146	ns
a vs. c (rel.; Fig. 4A)	<0.0001	***
b vs. c (rel.; Fig. 4A)	<0.0001	***
a vs. b (norm.; Fig. 4B)	0.9359	ns
a vs. c (norm.; Fig. 4B)	0.9936	ns
b vs. c (norm.; Fig. 4B)	0.9623	ns

(Table 3). Single bell-shaped concentration–response curves, including confidence intervals, means, and SEMs, are depicted in the SI (Fig. S6).

Efficacy and potency of TCDD exposure in specific co-transfection setups

All non-viral promoter setups were further tested in DLR assays after TCDD exposure, and data were fitted to nonlinear four-parameter log-logistic regression (4PL) with alterations described by (Weimer et al. 2012). In parallel to data of the BNF exposures above, both relative and normalized data outputs were computed and plotted. Concentration–response curves of the **pGL4.43 + pGL4.70**, **pGL4.43 + pRL-null**, and **pGudLuc7.5 + pRL-null[zfEF1aPro]** co-transfection setups are depicted below (Fig. 5), all other conducted test are shown in the SI (Fig. S8 and Tables S1+2). Initially, responses to TCDD exposure were tested since it is commonly used as a reference/positive control in toxicity testing, especially for deriving toxicity equivalents. In terms of efficacy, patterns were identical to the BNF exposure, with the **pGudLuc7.5 + pRL-null[zfEF1aPro]** combination depicting the most potent induction and plateauing at approximately 26-fold (Fig. 5A). Accordingly, the mean co-transfection setup effect differed statistically between all tested combinations

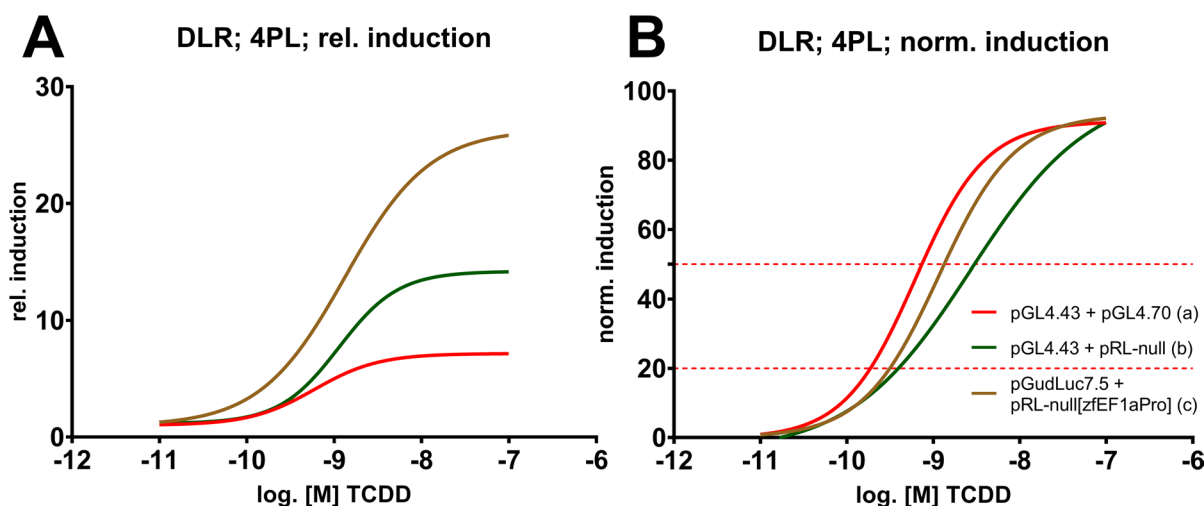


Fig. 5 Concentration–response curves of depicted co-transfection setups after TCDD exposure. Results of the DLR assays were either fitted as relative induction (A) or normalized induction values (B) to a four-parameter log-logistic

nonlinear regression (4PL). $EC_{20/50}$ values are summarized in Table 4. Specific concentration–response curves are illustrated in Fig. S8

(Table 5). Surprisingly, the **pGL4.43 + pGL4.70** depicted the highest potency (Fig. 5B and Table 4), differing statistically from **pGL4.43 + pRL-null** in terms of the overall effect of the normalized response (Table 5). Nevertheless, EC_{50} values (Table 4) differed only by approximately twofold and EC_{20} values were all recorded within the range of 200 pM. Further, these statements also account for all the other tested combinations, as depicted in the SI (Fig. S8 and Tables S1+2). Arguably, slight differences between co-transfection setups might rather be artefacts from manual titration and suboptimal nonlinear regression model-fit for some combinations. Thus, in terms of the TCDD exposure, using the **pGud-luc7.5 + pRL-null[zfEF1aPro]** co-transfection setup only increased the efficacy of the applied method but not the potency. In hindsight, directional cloning of the zfEF1a promoter into the **pGL4.70** normalization vector would have potentially added more information, given that after TCDD exposure, pGL4.70 vectors showed increased potency in co-transfection setups in comparison to **pRL-null** vectors (Table S1). Cytotoxicity was only recorded for the **pGud-luc7.5 + pRL-null[zfEF1aPro]** combination, which displayed none (Fig. S7). Further assessments of cellular viability were waived given that the non-viral promoter normalization vectors showed no additional cytotoxicity in the screening experiments and historical data displayed no TCDD-induced cytotoxicity within the same cellular context and within identical exposure concentrations (Eknefelt 2018).

BNF acts as a promiscuous activator of cellular stress response pathways

ZFL cells were also transiently co-transfected with the Nrf2-responsive reporter vector pGL4.37 and

Table 5 Comparison of mean co-transfection setup effects between combinations depicted in Fig. 5 and Table 4. Statistical significance in mean setup effects was assessed via two-way ANOVA, followed by Tukey's post hoc test (ns $P > 0.05$, ** $P < 0.01$, *** $P < 0.001$)

Comparison	Adjusted P -value	Significance
a vs. b (rel.; Fig. 5A)	0.0015	**
a vs. c (rel.; Fig. 5A)	< 0.0001	***
b vs. c (rel.; Fig. 5A)	< 0.0001	***
a vs. b (norm.; Fig. 5B)	0.0025	**
a vs. c (norm.; Fig. 5B)	0.2858	ns
b vs. c (norm.; Fig. 5B)	0.4350	ns

the normalization vector pRL-CMV, as described in (Lungu-Mitea and Lundqvist 2020). The transcription factor Nrf2 is a central regulator of the oxidative stress response pathways (Nrf2/Keap1/ARE) (Itoh et al. 2004) and a keystone in the regulation of oxidative stress detoxification, metabolism, and induction of related phase-II enzymes (e.g., GST, NQO1, HO-1). Detailed descriptions, results, and discussion are given in the respective section of the SI (p. 12–14; Figs. S10+11, Table S4). We recorded a LOEC of 30 nM and an EC_{50} of 9.7 nM within a BNF exposure range of 3 pM to 1 mM.

Discussion

The principal aim of this study was to develop a transient reporter gene assay of the AhR xenobiotic metabolism pathway in zebrafish hepatocytes, robust enough to be used in environmental testing. Within the introduction, we mentioned the potentials inherent to transient assays but also indicated issues that accompany transient transfection and might lead to artificial results (Stepanenko and Heng 2017;

Table 4 LOEC and $EC_{20/50}$ values derived from TCDD exposure (adj. R^2 and NRSME values are given as goodness-of-fit parameters of the nonlinear regression). According to setups depicted in Fig. 5

Transfection setup (according to Fig. 4)	LOEC (adj. P -value)	EC_{20} (normalized; adj. R^2 ; NRSME)	EC_{50} (normalized; adj. R^2 ; NRSME)	EC_{50} (relative; non-normalized; adj R^2 ; NRSME)	N (exp.)
(a) pGL4.43 + pGL4.70	100 pM (0.0406)	166 pM (0.88; 0.19)	612 pM (0.88; 0.19)	595 pM (0.57; 0.29)	8
(b) pGL4.43 + pRL-null	300 pM (0.008)	297 pM (0.85; 0.28)	2.70 nM (0.85; 0.28)	1.31 nM (0.47; 0.11)	6
(c) pGudLuc7.5 + pRL-null[zfEF1aPro]	100 pM (0.0003)	287 pM (0.92; 0.16)	1.15 nM (0.92; 0.16)	1.13 nM (0.62; 0.11)	8

Lungu-Mitea and Lundqvist 2020). Thus, the study's secondary aim was to disclose the origins of spurious expression or artificial signal inhibition that might originate from specific vector geometries. Zebrafish cells were chosen as a test model considering the zebrafish's progressively important role in toxicology, both in basic research and in testing (Garcia et al. 2016). Further, all xenobiotic metabolism pathway (AhR/ARNT/XRE) components are well described in zebrafish (Tanguay et al. 1999, 2000; Andreassen et al. 2002; Zeruth and Pollenz 2005, 2007; Hahn et al. 2017). The zebrafish liver cell line (ZFL) seemed an appropriate host for transfection of transient reporter vectors of the xenobiotic metabolism pathway, given that former research confirmed the presence of major components of the pathway in the permanent, immortal culture. Reports (Miranda et al. 1993; Ghosh and Collodi 1994; Ghosh et al. 1994) disclosed the activity of phase I xenobiotic metabolism enzymes of the cytochrome P450 (CYP) family on the proteomic level. Others (Henry et al. 2001; Evans et al. 2005; Eide et al. 2014) reported basal activity and induction capacity of the *zAhR2*, *zAhRR*, and *zCyp1A1* genes on the transcriptomic level. Beyond, one stable GFP-reporter (Mattingly et al. 2001) and one stable luciferase-reporter cell line (Yang et al. 2016; Chen and Chan 2017; Zhou et al. 2017) were derived from ZFL, demonstrating conservation and functionality of the AhR/ARNT/XRE xenobiotic metabolism response pathway.

Viral promoters squelch the AhR-related reporter signal in ZFL cells and induce size-dependent cytotoxicity

The primary results of the BNF-exposure screening on all sixteen tested co-transfection combinations revealed appropriate induction of the AhR-related signal only for the synthetic reporter construct on **pGL4.43** combined with minimal promoter bearing normalization vectors (Figs. 1, 2, S3, and S4). All co-transfection combinations utilizing viral promoters showed minimal induction of the AhR-related luminescence or none at all. Thereby, the reduced signal inductivity was correlated to the strength of the specific viral promoters (CMV > SV40 > TK; Fig. 2), as it was most apparent for the pRL-CMV vector, with a spurious upregulation of the Renilla luciferase (RLuc) normalization signal (Fig. 6B),

leading to a downregulation of the primary Firefly luciferase (FLuc) reporter signal (Fig. 6A). The pattern was not statistically significant for weaker viral promoters (data not plotted) or for any of the non-viral promoter co-transfection combinations involving the **pGudLuc7.5** reporter vectors. However, they were cognizable. Previously, we reported the conservation of viral promoter strength and associated transcription factors in the ZFL cell line (Lungu-Mitea and Lundqvist 2020). Nevertheless, the recorded luciferase signal has to be regarded in an integrative manner. Hence, an alteration of the reporter signal is not necessarily recordable by normalization signal upregulation. The phenomenon is defined as transcriptional “squelching” (Natesan et al. 1997), which refers to the competition between gene regulatory units for transcription factors, co-activators, and the overall transcription/translation machinery (Martino et al. 2004; Simon et al. 2015). Accordingly, viral promoter induced squelching has been reported for several cell lines, transfection constructs, and studied pathways (reviewed in Shifera and Hardin 2010; Stepanenko and Heng 2017)). Thereby, the effect cannot be generalized but depends on the utilized cellular context, the used transfection methods, the specific plasmid vector geometry, and the pathway studied (Mulholland et al. 2004; Lungu-Mitea and Lundqvist 2020). Correspondingly, we found the **pRL-CMV** normalization vector most potent in a co-transfection setup for assessing the induction of the Nrf2 cellular stress response pathway (Lungu-Mitea and Lundqvist 2020).

Except for the TK promoter, we once more (Lungu-Mitea and Lundqvist 2020) recorded a vector size-dependent increase in cytotoxicity when combining transient transfection with chemical exposure. SV40 and CMV-bearing vectors caused additional cytotoxicity compared to minP-containing vectors (Figs. S3+4; see Table 1 for vector size). Previous reports disclosed the vector-size dependent induction of the cellular immune response during transfection experiments (Jacobsen et al. 2009) and its interaction with the perceived signal (Ghazawi et al. 2005) by mimicking a viral infection due to the existence of exogenous, episomal genetic material (Terenzi et al. 1999). Such an induction will accelerate the inflammatory response and, thus, cytotoxicity. Interestingly, this effect was inverted by using the endogenous genomic *zEF1a* promoter (Fig. 2).

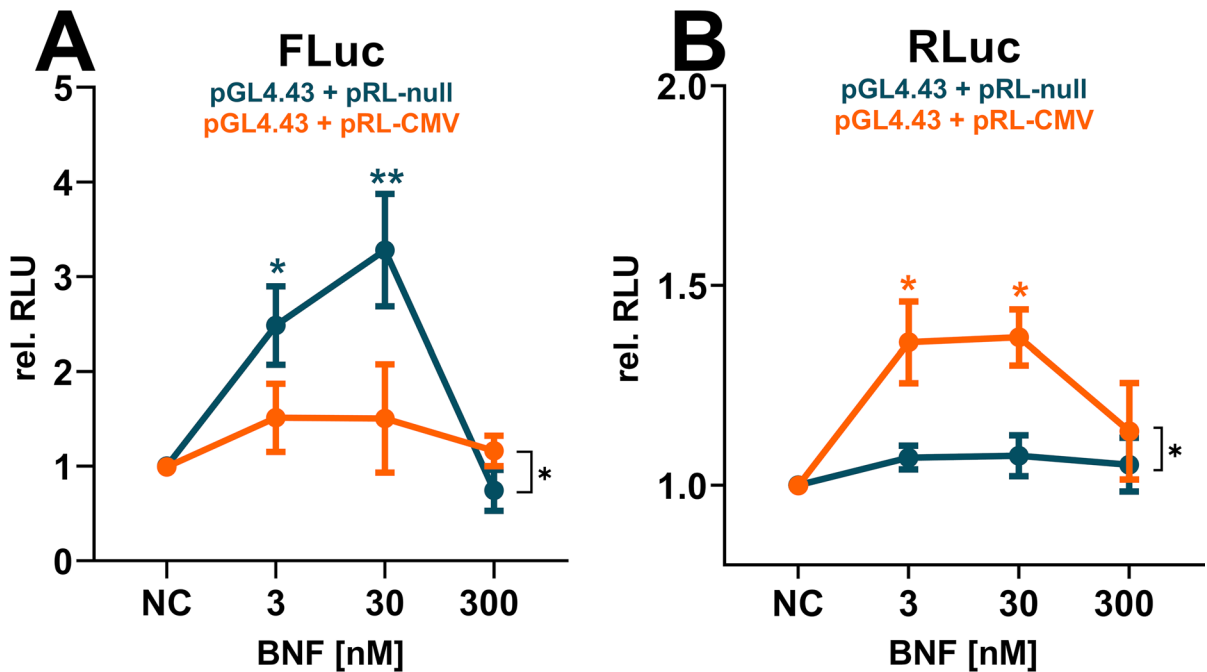


Fig. 6 Effects on relative raw luminescence units (rel. RLU) in the ZFL cell line exposed to BNF. Here, single luminescence signals are depicted: Firefly luciferase (FLuc) is the primary reporter signal derived from the expression of the reporter vector (A); Renilla luciferase (RLuc) is the normalization signal derived from the expression of the control vector (B). Mean relative RLU induction is illustrated as dots with whiskers,

including the SEM (experimental units $n=3-5$; observational units $N=9-15$). Colored asterisks indicate significance tested in a one-way ANOVA with Dunnett's post hoc test ($*P<0.05$, $**P<0.01$) within a specific co-transfection setup. Black asterisks indicate significance tested in a two-way ANOVA with Tukey's post hoc test ($*P<0.05$) to detect overall effects between co-transfection setups

Modulation of the luciferase reporter signal in transiently transfected ZFL cells after BNF and TCDD exposure

Except for the **pGudLuc7.5 + pRL-null[zfEFaprop]** co-transfection setup, which will be discussed in more detail further below, TCDD was the stronger AhR-agonist within all tested arrangements in comparison to BNF (see Tables 2 and 4). The latter statement is according to the literature, with the AhR showing greater affinity to the TCDD ligand in comparison to BNF (Soshilov and Denison 2014; Tagliabue et al. 2019). However, the ZFL system seems relatively insensitive to TCDD exposure with $EC_{20}S$ computed in the 200 pM range and $EC_{50}S$ in the 612 pM to 2.7 nM range, in regard to the co-transfection setup used (Tables 4 and S1). Mammalian reporter assays, especially rodent-derived cell lines, depict $EC_{50}S$ in the low pM range and limits of detection even within the fM range (Sanderson et al. 1996; Eichbaum et al.

2014). Apparently, mammalian-based assays are more sensitive to TCDD (rodent > human) and other dioxin-like compounds than fish-based assays (rainbow trout > zebrafish), due to structural differences and affinities of their respectively recruited AhRs (Abnet et al. 1999; Hilscherova et al. 2001; Keiter et al. 2008; Eichbaum et al. 2014). Even within fish, zebrafish is the most insensitive, commonly used test species, as demonstrated in vivo (Elonen et al. 1998; Jönsson et al. 2009; Doering et al. 2012) and in vitro (Creusot et al. 2014). Hence, the regulatory relevance of zebrafish-derived reporter assays of the AhR-regulated xenobiotic metabolism TP is in dispute. On the contrary, the system shows great potential in basic research and in vitro to in vivo extrapolation (IVIVE), given the wide acceptance of zebrafish in in vivo studies and the zebrafish embryo test (FET) (Braunbeck et al. 2005; Belanger et al. 2013).

Interestingly, we recorded a non-monotonous, bell-shaped (or bi-phasic) concentration–response

curve (NMCRC) after BNF exposure. Thereby, the inhibition was not dependent on the co-transfection setup, with all tested setups showing approximate PC_{max}^s (15.7–19.5 nM) and IC_{50}^s (27–109 nM, see Table 2). Hence, a common, non-transfection related mechanism might be responsible for the downregulation, and cytotoxicity has been ruled out. The AhR is promiscuous and binds to various ligand classes with different affinities (Soshilov and Denison 2014). Other classes of ligands might also alternate translocator recruitment. Within the AhR/ARNT/XRE pathway, upon activation by specific classes of ligands, AhR can dimerize with alternating co-factors to act as a transcription factor in non-canonical pathways (reviewed in Denison and Faber 2017; Wright et al. 2017)).

Josyula et al. (2020) mapped the entire AhR-mediated transcriptional regulatory network and identified many endogenous functions such as lipid metabolism, cellular immune response, and cell migration. Further, they found direct and combinatorial control (“tethering”) of gene expression of various cellular stress response pathways by AhR. TPs of the xenobiotic metabolism (PXR, PPAR, AhR), the hormone response (ER, AR, GR), and the cellular stress response (Nrf2, p53, HIF-1, NfκB, MTF, among others) are known to exhibit crosstalk within their specific domains due to a commonly shared structural architecture (reviewed in Simmons et al. 2009; Lushchak 2011)). However, an increasing body of literature indicates the existence of generalized crosstalk between all primary TPs. Among others, AhR has been found to interact with the ER (Safe 1995; Safe et al. 1998; Klinge et al. 2000; Ohtake et al. 2003; Cheshenko et al. 2006), Nrf2 (Ma et al. 2004; Miao et al. 2005; Köhle and Bock 2007; Shin et al. 2007; Yeager et al. 2009; Raghunath et al. 2018), and NfκB (Schlezingner et al. 2000a; Tian 2009) TPs. Additionally, a close structural architecture to the hypoxia-inducible factor 1 (HIF1) pathway (Schmidt and Bradfield 1996; Andreassen et al. 2002; Simmons et al. 2009) locates AhR close to the stress response pathways. Regarding cellular stress response pathways, the transcription factors are mostly pathway-specific; however, transducers and translocators are often shared, enabling a rapid response to stressors by mounting the cellular defence mechanisms on multiple ends (Simmons et al. 2009; Lushchak 2011). Such a multiple upregulation may either be encountered at once, close to concentrations causing cytotoxicity

(termed “avalanche effect” or “toxicity burst” (Escher et al. 2013; Judson et al. 2016)), or in an orchestral manner with one stressor activating different pathways at different effect concentrations (Simmons et al. 2009; Lushchak 2011).

We retrieved ToxCast database outputs via the CompTox dashboard (<https://comptox.epa.gov/dashboard>) for BNF and encountered positive hits for diverse TPs (Fig. S9 and Table S3) ahead of the cytotoxicity cutoff. Many of the major TPs of the xenobiotic metabolism (AhR, RAR, PPAR, PXR), hormone response (ER, AR, VDR), and cellular stress response (Nrf2) are activated by BNF exposure in the mid nM to lower μM scale. ER, AhR, and Nrf2-related bioassays depicted top-scale induction. Interestingly, the histone deacetylase inhibitor (HDACi) epigenetic marker showed a notable upregulation, indicating a general impact on gene regulation. Additionally, we decided to test the induction of the Nrf2 cellular stress response pathway in the ZFL cell line after exposure to BNF by employing a previously described DLR reporter gene assay (Lungu-Mitea and Lundqvist 2020). For more details, see the respective section in the SI (Figs. S10+11; Table S4). Interestingly, we saw maximal Nrf2 induction at 100 nM BNF (Fig. S10) coinciding with concentrations triggering an AhR inhibition (e.g., Figs. 1 and 3). Further, we computed an EC_{50} for Nrf2 induction at 9.7 nM (Fig. S11 and Table S4), which coincides with PC_{max}^s of the NMCRCs in the range of 15.7 to 19.5 nM. Taken together, BNF most likely acts as an inducer of multiple TPs. Figure 7 depicts how NMCRC might be modulated via squelching by BNF promiscuously activating multiple toxicity pathways.

Accordingly, NMCRCs were also recorded after BNF exposure in zebrafish embryos (Noury et al. 2006), adult guppy (Frasco and Guilhermino 2002), and rainbow trout hepatocytes (RTL-W1; (Heinrich et al. 2014)) but so far lacked explanation. Beyond, non-monotonicity was also encountered after exposure to various dioxin-like compounds (DLCs) and polycyclic aromatic hydrocarbons (PAHs) when recording CYP1A1 activity via the EROD-assay, in both in vivo and in vitro test systems, at non-cytotoxic concentrations, and in various species (Gooch et al. 1989; Hahn et al. 1993, 1996; Hahn and Chandran 1996; Verhallen et al. 1997; White et al. 1997; Delescluse et al. 1997; Tysklind et al. 1998; Schlezingner et al. 1999, 2000b, 2006; Wassenberg et al. 2005). Thereby, NMCRCs

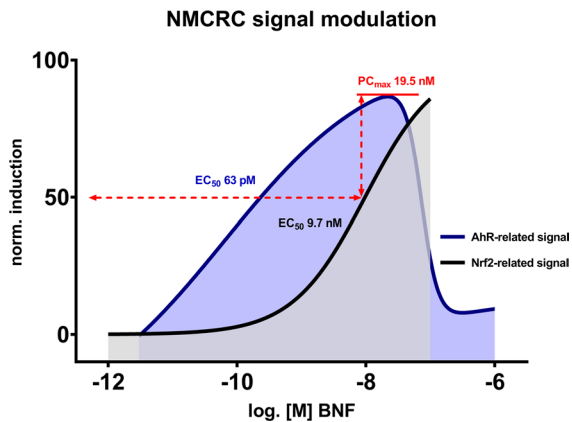


Fig. 7 Schematic illustration of BNF-induced CRCs in a xenobiotic metabolism (AhR) and oxidative stress (Nrf2)-related transient reporter gene assay in ZFL cells. Hypothetically, NMCRCs, as recorded for the AhR-related signal, are due to TPs squelching or feedback loop mechanisms, given BNF's promiscuity. Consult Figs. S6C and S11 for actual CRC-fits

were limited to CYP1A1 activity recorded via the EROD-assay, whereas total CYP1A1 protein amounts (Hahn et al. 1993) and mRNA transcript levels (White et al. 1997; Delescluse et al. 1997) were either stable or increasing with increasing exposure concentrations. A few possible explanations of the phenomenon were proposed: inhibition of heme synthesis and uroporphyrin (Hahn and Chandran 1996; Tysklind et al. 1998), competitive inhibition of the EROD enzyme–substrate reaction by DLCs and PAHs (Petrucci and Bunce 1999), or uncoupling of the CYP1A1 catalytic cycle by respective compounds resulting in ROS formation within the active site (White et al. 1997; Schlezinger et al. 1999, 2000b, 2006). Further, ROS were associated with a downregulation of overall CYP1A1 amount and activity (White et al. 1997; Xu and Pasco 1998; Schlezinger et al. 1999).

In this study, we saw NMCRCs after BNF but not after TCDD exposure. To our knowledge, there is no literature interpreting such a phenomenon for flavonoids or polyphenols, but similar mechanisms seem plausible due to structural proximities to DLCs and PAHs (abbreviations given in SI). Only sigmoidal concentration–response curves were recorded here after TCDD exposure. Theoretically, NMCRCs would also be encountered here if exposure regimes were appropriately extended. However, worth mentioning, maximal exposure concentrations in this

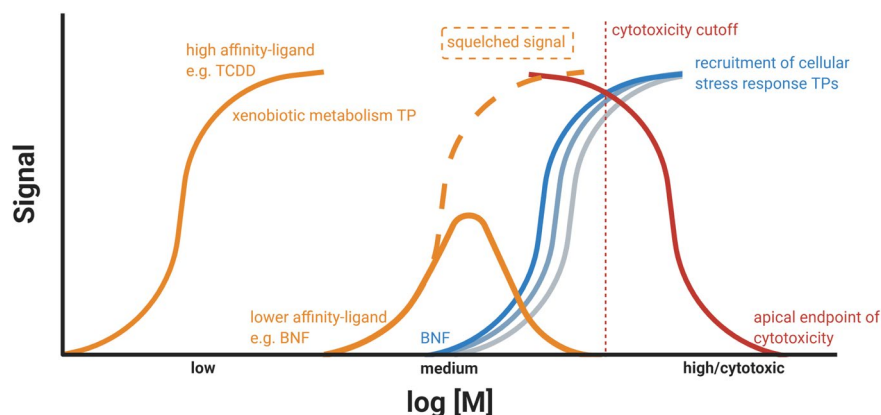
study were operating close to the onset of TCDD-induced cytotoxicity in ZFL cell lines (Eknefelt 2018). Thus, the latter would have superimposed a potential NMCRC.

Taken together, we cannot precisely define if downregulation of the AhR/ARNT/XRE pathway for NMCRCs materializes on the level of transactivation, transcription, or translation, as such was not the purpose of the study. Instead, we hypothesize a squelching phenomenon, given the promiscuous induction of TPs by BNF on the gene transactivation level, coinciding at specific EC_{50} , IC_{50} , and PC_{max} concentrations. The presented data adds crucial information on the appearance of NMCRCs after BNF exposure. However, further investigation will be necessary to pinpoint its core mechanism. Given the existence of generalized crosstalk between all primary TPs, as discussed above, it is, however, plausible that interactions originate on the level of transactivation. Hypothetically, negative feedback loops from uncoupling-derived ROS (White et al. 1997; Xu and Pasco 1998; Schlezinger et al. 1999) or alternate modulation of mRNA transcript stability (Zhao et al. 2021) are other vital explanations. We want to advocate here that the encountered NMCRCs might be a result of squelching between multiple TPs recruiting the transcription/translation machinery simultaneously (Fig. 8), as indicated by our data and ToxCast outputs. The transactivation of multiple TPs by single compounds has been rigorously described (Kamei et al. 1996; Xu and Pasco 1998; Klinge et al. 2000; Schlezinger et al. 2000a; Ma et al. 2004; Miao et al. 2005; Köhle and Bock 2007; Shin et al. 2007; Yeager et al. 2009; Kalthoff et al. 2010; Ulin et al. 2019). However, we cannot identify if BNF acts *a priori* as a multiple inducer or if an original signal is sequestered into numerous responses. Conclusively, recorded patterns are a linear, one-dimensional snapshot of a multi-dimensional feature.

The zEF1a genomic promoter rescues the luciferase signal from “maisonette squelching”

It is recommended to test reporter gene assays containing synthetic and genomic promoters to respectively account for differences in specificity and sensitivity (Simmons et al. 2009). In terms of reporter vectors, we utilized both types with **pGL4.43**

Fig. 8 Schematic representation of the hypothetical squelching of the AhR TP-related luciferase signal (orange) due to activation of alternate cellular stress response pathways (shades of blue) in a system under increasing toxic stress, up to cytotoxicity (red). The illustration was generated in BioRender



(synthetic) and **pGudLuc7.5** (genomic). Further, we designed a novel normalization vector **pRL-null[zfEF1aPro]** by directional cloning of the zebrafish translational elongation factor 1a promoter, a highly active genomic promoter (Gao et al. 1997), into the multiple cloning site of the **pRL-null** plasmid. Reporter cassettes employing the EF1a promoter were reported to enable a robust and constant expression of desired episomal target genes and, beyond, were not prone to gene-silencing once applied in stable transfection (Gopalkrishnan et al. 1999; Wang et al. 2017). Above, we established how strong viral promoters squelched the luciferase signal (Figs. 2 + 6) and potentially introduced cytotoxicity via inflammation (Figs. S3 + S4). On the contrary, a genomic promoter is less likely to be considered exogenous material by the cellular immune response. It might be regulated natively by the cellular transcription/translation machinery, thus, not being prone to spurious up and downregulation. Beyond, viral promoters often bear cryptic binding sites, such as for the activator protein 1 (AP1) transcription factor (Kushner et al. 1994; Grimm and Nordeen 1999; Hall et al. 2002; Dougherty and Sanders 2005). The latter regulates manifold gene expression in the context of cellular metabolism and homeostasis, as it is associated with the MAPK pathways (Swanson et al. 1995; Shifera and Hardin 2009). Within a stressed system, AP1 will be alternatively regulated and impact the expression of episomal target genes on plasmid vectors fused to viral promoters. On the contrary, genomic EF1a promoter bear reduced cryptic binding sites compared to viral promoters (Wang et al. 2017), making them less susceptible to spurious regulation within a stressed system.

In this study, we encountered a complete rescue of the AhR-mediated signal when applying the **pGudLuc7.5 + pRL-null[zfEF1aPro]** co-transfection setup (Figs. 1, 2, and 3). Beyond, we recorded an overall increase in efficacy and partly in potency (Figs. 4 and 5) for the genomic reporter construct **pGudLuc7.5**. However, those enhancements were only marginally encountered when using the **pGL4.43 + pRL-null[zfEF1aPro]** co-transfection setup (Fig. S5). Apparently, by utilizing the zfEF1a genomic promoter, vector-mediated squelching based on strong viral promoters was omitted. Further, an inflammatory response of the cell line due to transfection was most likely avoided due to the genomic promoter's endogenous nature. In parallel to our study, other studies confirmed ROS-mediated transcriptional suppression of the AhR/ARNT/XRE TP in dependency of the inducible transcriptional strength of XREs within their respective reporter gene cassettes (Xu and Pasco 1998). Thereby, conditions that increased the transactivation potential of AhR attenuated the action of ROS, whereas conditions that reduced XRE-mediated transactivation potentiated the inhibitory action of ROS. Identically, we saw a complete inhibition of transactivation for unfitting co-transfection combinations (e.g., Fig. 1C).

In theory, we regard the more or less complete initial silencing of the **pGudLuc7.5** (Figs. 1 and 2) reporter vector as squelching on multiple levels: Firstly, on the level of plasmid-bound gene-regulatory units competing with each other and episomal target genes for the recruitment of transcription factors and co-factors (Fig. 6). Secondly, on the level of competing TPs for the same machinery as an overall detoxification response (Figs. 7 and 8). Prospectively,

we want to declare and address such a multi-level squelching phenomenon, as it can be observed in transiently transfected systems under stress as “maisonette squelching.” As follows, we assume that the slight increase in potency after co-transfection with **pRL-null[zfEF1a]** results from less competition between reporter and normalization vector (Fig. 5B). Further, we saw a strong increase in efficacy for **pGudLuc7.5 + pRL-null[zfEF1aPro]** (Figs. 3 and 5A) but not for **pGL4.43 + pRL-null[zfEF1aPro]** (Fig. S5). Apparently, **pGL4.43** was not squelched in combination with the minP-bearing normalization vectors, whereas it was the case for **pGudLuc7.5**. Hence, the utilization of a genomic promoter did not alter expression patterns significantly for the letter. However, **pGudLuc7.5** profited substantially from co-transfection with **pRL-null[zfEF1aPro]**. We assume the increase in efficacy to be based on the higher amount of XREs (twenty within the promoter cassette of **pGudLuc7.5**) compared to the synthetic promoter (three on **pGL4.43**; see also Table 1). Thus, once **pGudLuc7.5** is not squelched on the primary level, it can recruit a higher amount of AhR/ARNT and express the reporter gene more efficiently (see also paragraph above).

Conclusion

Here, we report the development of an AhR-responsive transient reporter assay in the ZFL cell line by applying previously conceived technologies and strategies. Further, we report the vector geometry-induced squelching of the primary reporter signal by viral, constitutive promoters. Beyond, we designed a novel normalization vector, bearing an endogenous zebrafish-derived genomic promoter (zfEF1aPro), which rescues the squelching-delimited system, thus, giving new insights into the modulation of transient reporter systems under xenobiotic stress. Additionally, we confirmed *in vivo* results of the xenobiotic metabolism TP in zebrafish. Seemingly, zebrafish-derived systems are intrinsically low responders to AhR-mediated effects of dioxin-like compounds. Hence, their applicability is disputable in terms of predicting low-dose effects but valuable in mechanistic terms. Finally, we uncovered how the ubiquitously used ligand BNF promiscuously activates TPs of the xenobiotic metabolism and cellular stress response in an orchestral manner, leading to a

concentration-related inhibition of the AhR/ARNT/XRE-TP and NMCRCs. We named such a multi-level inhibitory mechanism that might mask effects as “maisonette squelching.”

Abbreviations Most abbreviations are defined upon the first appearance, with some familiar exceptions. A detailed list of abbreviations is given in the supplementary information file (SI)

Acknowledgements The authors are grateful to Dr. Patrick Heinrich, Center for Biochemistry, University of Heidelberg, and Prof. Dr. Michael Denison, Department of Environmental Toxicology, University of California, for generous research material gifts. Further, we thank Dr. Mark Hahn, Woods Hole Oceanographic Institution, and Dr. Maria Jönsson, Department of Organismal Biology, University of Uppsala, for sharing scientific insights and literature. Finally, we would like to thank Prof. Dr. Agneta Oskarsson, Department of Biomedicine and Veterinary Public Health, SLU Uppsala, for reviewing and Matilda Stein Åslund, Department of Forest Mycology and Plant Pathology, SLU Uppsala, for proofreading the manuscript.

Author contribution Conceptualization: Sebastian Lungu-Mitea and Johan Lundqvist; Methodology: Yuxin Han and Sebastian Lungu-Mitea; Formal analysis and investigation: Sebastian Lungu-Mitea; Writing – original draft preparation: Sebastian Lungu-Mitea; Writing – review and editing: Johan Lundqvist, Sebastian Lungu-Mitea, and Yuxin Han; Funding acquisition: Johan Lundqvist; Resources: Johan Lundqvist; Supervision: Johan Lundqvist.

Funding Open access funding provided by Swedish University of Agricultural Sciences. This work was financially supported by the Swedish Research Council (grant no. 2015–03404), the Research Council Formas (grant no. 2014–1435), the Royal Swedish Academy of Agriculture and Forestry (grant no. H14-0162-CHF), and the Swedish Fund for Research Without Animal Experiments (grant no. N2016-0007).

Data availability All data generated or analyzed during this study are included in this published article (and its supplementary files). Raw data are available from the corresponding author upon request.

Code availability Not applicable.

Declarations

Ethics approval Not applicable; the manuscript does not contain clinical studies, patient data, or animal experiments.

Consent to participate Not applicable.

Consent for publications Not applicable.

Conflict of interest The authors declare no competing interests.

Open Access This article is licensed under a Creative Commons Attribution 4.0 International License, which permits use, sharing, adaptation, distribution and reproduction in any medium or format, as long as you give appropriate credit to the original author(s) and the source, provide a link to the Creative Commons licence, and indicate if changes were made. The images or other third party material in this article are included in the article's Creative Commons licence, unless indicated otherwise in a credit line to the material. If material is not included in the article's Creative Commons licence and your intended use is not permitted by statutory regulation or exceeds the permitted use, you will need to obtain permission directly from the copyright holder. To view a copy of this licence, visit <http://creativecommons.org/licenses/by/4.0/>.

References

- Abnet CC, Tanguay RL, Heideman W, Peterson RE. Trans-activation activity of human, zebrafish, and rainbow trout aryl hydrocarbon receptors expressed in COS-7 cells: greater insight into species differences in toxic potency of polychlorinated dibenzo-p-dioxin, dibenzofuran, and biphenyl congeners. *Toxicol Appl Pharmacol*. 1999;159:41–51. <https://doi.org/10.1006/taap.1999.8719>.
- Andreasen EA, Hahn ME, Heideman W, et al. The zebrafish (*Danio rerio*) aryl hydrocarbon receptor type 1 is a novel vertebrate receptor. *Mol Pharmacol*. 2002;62:234–49. <https://doi.org/10.1124/mol.62.2.234>.
- Ankley G, Mihaich E, Stahl R, et al. Overview of a workshop on screening methods for detecting potential (anti-) estrogenic/androgenic chemicals in wildlife. *Environ Toxicol Chem*. 1998;17:68–87. <https://doi.org/10.1002/etc.5620170110>.
- Ankley GT, Bennett RS, Erickson RJ, et al. Adverse outcome pathways: a conceptual framework to support ecotoxicology research and risk assessment. *Environ Toxicol Chem*. 2010;29:730–41. <https://doi.org/10.1002/etc.34>.
- Belanger SE, Rawlings JM, Carr GJ. Use of fish embryo toxicity tests for the prediction of acute fish toxicity to chemicals. *Environ Toxicol Chem*. 2013;32:1768–83. <https://doi.org/10.1002/etc.2244>.
- Brack W, Ait-Aissa S, Altenburger R, et al. Let us empower the WFD to prevent risks of chemical pollution in European rivers and lakes. *Environ Sci Eur*. 2019;31:47. <https://doi.org/10.1186/s12302-019-0228-7>.
- Brack W, Dulio V, Ågerstrand M, et al. Towards the review of the European Union Water Framework Directive: recommendations for more efficient assessment and management of chemical contamination in European surface water resources. *Sci Total Environ*. 2017;576:720–37. <https://doi.org/10.1016/j.scitotenv.2016.10.104>.
- Brack W, Escher BI, Müller E, et al. Towards a holistic and solution-oriented monitoring of chemical status of European water bodies: how to support the EU strategy for a non-toxic environment? *Environ Sci Eur*. 2018;30:33. <https://doi.org/10.1186/s12302-018-0161-1>.
- Braunbeck T, Boettcher M, Hollert H, et al. Towards an alternative for the acute fish LC(50) test in chemical assessment: the fish embryo toxicity test goes multi-species – an update. *Altex*. 2005;22:87–102.
- Carvan MJ 3rd, Solis WA, Gedamu L, Nebert DW. Activation of transcription factors in zebrafish cell cultures by environmental pollutants. *Arch Biochem Biophys*. 2000;376:320–7. <https://doi.org/10.1006/abbi.2000.1727>.
- Chen YY, Chan KM. Transcriptional inhibition of TCDD-mediated induction of cytochrome P450 1A1 and alteration of protein expression in a zebrafish hepatic cell line following the administration of TCDD and Cd 2+. *Toxicol Lett*. 2017. <https://doi.org/10.1016/j.toxlet.2017.10.017>.
- Cheshenko K, Brion F, Le Page Y, et al. Expression of zebra fish aromatase cyp19a and cyp19b genes in response to the ligands of estrogen receptor and aryl hydrocarbon receptor. *Toxicol Sci*. 2006;96:255–67. <https://doi.org/10.1093/toxsci/kfm003>.
- Collins FS, Gray GM, Bucher JR. Transforming environmental health protection. *Science* (80-). 2008;319:906–7. <https://doi.org/10.1126/science.1154619>.
- Creusot N, Brion F, Piccini B, et al. BFCOD activity in fish cell lines and zebrafish embryos and its modulation by chemical ligands of human aryl hydrocarbon and nuclear receptors. *Environ Sci Pollut Res*. 2014;22:16393–404. <https://doi.org/10.1007/s11356-014-3882-8>.
- Delescluse C, Ledirac N, de Sousa G, et al. Comparative study of CYP1A1 induction by 3-methylcholanthrene in various human hepatic and epidermal cell types. *Toxicol In Vitro*. 1997;11:443–50. [https://doi.org/10.1016/S0887-2333\(97\)00077-5](https://doi.org/10.1016/S0887-2333(97)00077-5).
- Denison MS, Faber SC. And now for something completely different: diversity in ligand-dependent activation of Ah receptor responses. *Curr Opin Toxicol*. 2017;2:124–31. <https://doi.org/10.1016/j.cotox.2017.01.006>.
- Denison MS, Fisher JM, Whitlock JP. Protein-DNA interactions at recognition sites for the dioxin-Ah receptor complex. *J Biol Chem*. 1989;264:16478–82.
- Doering J, a, Wiseman S, Beitel SC, et al. Tissue specificity of aryl hydrocarbon receptor (AhR) mediated responses and relative sensitivity of white sturgeon (*Acipenser transmontanus*) to an AhR agonist. *Aquat Toxicol*. 2012;114–115:125–33. <https://doi.org/10.1016/j.aquatox.2012.02.015>.
- Dougherty DC, Sanders MM. Comparison of the responsiveness of the pGL3 and pGL4 luciferase reporter vectors to steroid hormones. *Biotechniques*. 2005;39:203–7. <https://doi.org/10.2144/05392ST02>.
- Eichbaum K, Brinkmann M, Buchinger S, et al. In vitro bioassays for detecting dioxin-like activity — application potentials and limits of detection, a review. *Sci Total Environ*. 2014;487:37–48. <https://doi.org/10.1016/j.scitotenv.2014.03.057>.
- Eide M, Rusten M, Male R, et al. A characterization of the ZFL cell line and primary hepatocytes as in vitro liver cell models for the zebrafish (*Danio rerio*). *Aquat Toxicol*. 2014;147:7–17. <https://doi.org/10.1016/j.aquatox.2013.11.023>.

- Eknefelt L. Nya metoder för att detektera AhR-aktivitet i fiskceller. Sveriges lantbruksuniversitet. 2018.
- El-Fouly MH, Richter C, Giesy JP, Denison MS. Production of a novel recombinant cell line for use as a bioassay system for detection of 2,3,7,8-tetrachlorodibenzo-*P*-dioxin-like chemicals. *Environ Toxicol Chem*. 1994;13:1581–8. <https://doi.org/10.1002/etc.5620131006>.
- Elonen GE, Spehar RL, Holcombe GW, et al. Comparative toxicity of 2,3,7,8-tetrachlorodibenzo-*p*-dioxin to seven freshwater fish species during early life-stage development. *Environ Toxicol Chem*. 1998;17:472–83. <https://doi.org/10.1002/etc.5620170319>.
- Escher BI, van Daele C, Dutt M, et al. Most oxidative stress response in water samples comes from unknown chemicals: the need for effect-based water quality trigger values. *Environ Sci Technol*. 2013;47:7002–11. <https://doi.org/10.1021/es304793h>.
- EURL-ECVAM. EURL ECVAM Status Report on the Development, Validation and Regulatory Acceptance of Alternative Methods and Approaches. 2014.
- Evans BR, Karchner SI, Franks DG, Hahn ME. Duplicate aryl hydrocarbon receptor repressor genes (*ahrr1* and *ahrr2*) in the zebrafish *Danio rerio*: structure, function, evolution, and AHR-dependent regulation in vivo. *Arch Biochem Biophys*. 2005;441:151–67. <https://doi.org/10.1016/j.abb.2005.07.008>.
- Frasco MF, Guilhermino L. Effects of dimethoate and beta naphthoflavone on selected biomarkers of *Poecilia reticulata*. *Fish Physiol Biochem*. 2002;26:149–56. <https://doi.org/10.1023/A:1025457831923>.
- Gao D, Li Z, Murphy T, Sauerbier W. Structure and transcription of the gene for translation elongation factor 1 subunit alpha of zebrafish (*Danio rerio*). *Biochim Biophys Acta. - Gene Struct Expr*. 1997;1350:1–5. [https://doi.org/10.1016/S0167-4781\(96\)00179-0](https://doi.org/10.1016/S0167-4781(96)00179-0).
- Garcia GR, Noyes PD, Tanguay RL. Advancements in zebrafish applications for 21st century toxicology. *Pharmacol Ther*. 2016;161:11–21. <https://doi.org/10.1016/j.pharmthera.2016.03.009>.
- Garrison PM, Tullis K, Aarts JM, et al. Species-specific recombinant cell lines as bioassay systems for the detection of 2,3,7,8-tetrachlorodibenzo-*p*-dioxin-like chemicals. *Fundam Appl Toxicol*. 1996;30:194–203.
- Ghazawi I, Cutler SJ, Low P, et al. Inhibitory effects associated with use of modified *Photinus pyralis* and *Renilla reniformis* luciferase vectors in dual reporter assays and implications for analysis of ISGs. *J Interferon Cytokine Res*. 2005;25:92–102. <https://doi.org/10.1089/jir.2005.25.92>.
- Ghosh C, Collodi P. Culture of cells from zebrafish (*Brachydanio rerio*) blastula-stage embryos. *Cytotechnology*. 1994;14:21–6. <https://doi.org/10.1007/BF00772192>.
- Ghosh C, Zhou YL, Collodi P. Derivation and characterization of a zebrafish liver cell line. *Cell Biol Toxicol*. 1994;10:167–76. <https://doi.org/10.1007/BF00757560>.
- Giani Tagliabue S, Faber SC, Motta S, et al. Modeling the binding of diverse ligands within the Ah receptor ligand binding domain. *Sci Rep*. 2019;9:10693. <https://doi.org/10.1038/s41598-019-47138-z>.
- Goldberg AM. The principles of humane experimental technique: is it relevant today? *Altex*. 2010;27:25–7.
- Gooch JW, Elskus AA, Kloeppe-Sams PJ, et al. Effects of ortho- and non-ortho-substituted polychlorinated biphenyl congeners on the hepatic monooxygenase system in scup (*Stenotomus chrysops*). *Toxicol Appl Pharmacol*. 1989;98:422–33. [https://doi.org/10.1016/0041-008X\(89\)90171-3](https://doi.org/10.1016/0041-008X(89)90171-3).
- Gopalkrishnan RV, Christiansen KA, Goldstein NI, et al. Use of the human EF-1 α promoter for expression can significantly increase success in establishing stable cell lines with consistent expression: a study using the tetracycline-inducible system in human cancer cells. *Nucleic Acids Res*. 1999;27:4775–82. <https://doi.org/10.1093/nar/27.24.4775>.
- Green JW, Springer TA, Holbech H. Statistical analysis of ecotoxicity studies. Hoboken: John Wiley & Sons Inc; 2018.
- Grimm SL, Nordeen SK. Luciferase reporter gene vectors that lack potential AP-1 sites. *Biotechniques*. 1999;27:220–2. <https://doi.org/10.2144/99272bm01>.
- Hahn ME, Chandran K. Uroporphyrin accumulation associated with cytochrome P4501A induction in fish hepatoma cells exposed to aryl hydrocarbon receptor agonists, including 2,3,7,8-tetrachlorodibenzo-*p*-dioxin and planar chlorobiphenyls. *Arch Biochem Biophys*. 1996;329:163–74. <https://doi.org/10.1006/abbi.1996.0205>.
- Hahn ME, Karchner SI, Merson RR. Diversity as opportunity: insights from 600 million years of AHR evolution. *Curr Opin Toxicol*. 2017;2:58–71. <https://doi.org/10.1016/j.cotox.2017.02.003>.
- Hahn ME, Lamb TM, Schultz ME, et al. Cytochrome P4501A induction and inhibition by 3,3',4,4'-tetrachlorobiphenyl in an Ah receptor-containing fish hepatoma cell line (PLHC-1). *Aquat Toxicol*. 1993;26:185–208. [https://doi.org/10.1016/0166-445X\(93\)90030-5](https://doi.org/10.1016/0166-445X(93)90030-5).
- Hahn ME, Woodward BL, Stegeman JJ, Kennedy SW. Rapid assessment of induced cytochrome P4501A protein and catalytic activity in fish hepatoma cells grown in multi-well plates: response to TCDD, TCDF, and TWO planar PCBs. *Environ Toxicol Chem*. 1996;15:582. [https://doi.org/10.1897/1551-5028\(1996\)015%3c0582:RAOICP%3e2.3.CO;2](https://doi.org/10.1897/1551-5028(1996)015%3c0582:RAOICP%3e2.3.CO;2).
- Halder M, Kienzler A, Whelan M, Worth A. EURL ECVAM Strategy to replace, reduce and refine the use of fish in aquatic toxicity and bioaccumulation testing. 2014.
- Hall M-C, Young DA, Rowan AD, et al. Cryptic promoter activity of pBLCAT3 induced by overexpression of AP1 factors. *Biotechniques*. 2002;33:1004, 1006, 1008.
- Han D, Nagy SR, Denison MS. Comparison of recombinant cell bioassays for the detection of Ah receptor agonists. *BioFactors*. 2004;20:11–22. <https://doi.org/10.1002/biof.5520200102>.
- Hartung T. Lessons learned from alternative methods and their validation for a new toxicology in the 21st century. *J Toxicol Environ Health B Crit Rev*. 2010;13:277–90. <https://doi.org/10.1080/10937404.2010.483945>.
- Hartung T. From alternative methods to a new toxicology. *Eur J Pharm Biopharm*. 2011;77:338–49. <https://doi.org/10.1016/j.ejpb.2010.12.027>.
- He G, Tsutsumi T, Zhao B, et al. Third-generation Ah receptor-responsive luciferase reporter plasmids: amplification of dioxin-responsive elements dramatically increases CALUX

- bioassay sensitivity and responsiveness. *Toxicol Sci.* 2011;123:511–22. <https://doi.org/10.1093/toxsci/kfr189>.
- Heinrich P, Braunbeck T. Genetically engineered zebrafish liver (ZF-L) cells as an in vitro source for zebrafish acetylcholinesterase (zfAChE) for the use in AChE inhibition assays. *Toxicol In Vitro.* 2018;#pagerange#. <https://doi.org/10.1016/j.tiv.2018.06.003>.
- Heinrich P, Diehl U, Förster F, Braunbeck T. Improving the in vitro ethoxresorufin-O-deethylase (EROD) assay with RTL-W1 by metabolic normalization and use of β -naphthoflavone as the reference substance. *Comp Biochem Physiol Part C Toxicol Pharmacol.* 2014;164:27–34. <https://doi.org/10.1016/j.cbpc.2014.04.005>.
- Henry TR, Nesbit DJ, Heideman W, Peterson RE. Relative potencies of polychlorinated dibenzo-p-dioxin, dibenzofuran, and biphenyl congeners to induce cytochrome P4501A mRNA in a zebrafish liver cell line. *Environ Toxicol Chem.* 2001;20:1053–8. <https://doi.org/10.1002/etc.5620200516>.
- Hilscherova K, Kannan K, Kang Y-S, et al. Characterization of dioxin-like activity of sediments from a Czech River Basin. *Environ Toxicol Chem.* 2001;20:2768–77. <https://doi.org/10.1002/etc.5620201216>.
- Itoh K, Tong KI, Yamamoto M. Molecular mechanism activating Nrf2-Keap1 pathway in regulation of adaptive response to electrophiles. *Free Radic Biol Med.* 2004;36:1208–13. <https://doi.org/10.1016/j.freeradbiomed.2004.02.075>
- Jacobsen LB, Calvin SA, Lobenhofer EK. Transcriptional effects of transfection: the potential for misinterpretation of gene expression data generated from transiently transfected cells. *Biotechniques.* 2009;47:617–24. <https://doi.org/10.2144/000113132>.
- Jönsson ME, Brunström B, Brandt I. The zebrafish gill model: induction of CYP1A, EROD and PAH adduct formation. *Aquat Toxicol.* 2009;91:62–70. <https://doi.org/10.1016/j.aquatox.2008.10.010>.
- Josyula N, Andersen ME, Kaminski NE, et al. Gene co-regulation and co-expression in the aryl hydrocarbon receptor-mediated transcriptional regulatory network in the mouse liver. *Arch Toxicol.* 2020;94:113–26. <https://doi.org/10.1007/s00204-019-02620-5>.
- Judson R, Houck K, Martin M, et al. Editor's Highlight: Analysis of the effects of cell stress and cytotoxicity on in vitro assay activity across a diverse chemical and assay space. *Toxicol Sci.* 2016;152:323–39. <https://doi.org/10.1093/toxsci/kfw092>.
- Kalthoff S, Ehmer U, Freiberg N, et al. Interaction between oxidative stress sensor Nrf2 and xenobiotic-activated aryl hydrocarbon receptor in the regulation of the human phase II detoxifying UDP-glucuronosyltransferase 1A10. *J Biol Chem.* 2010;285:5993–6002. <https://doi.org/10.1074/jbc.M109.075770>.
- Kamei Y, Xu L, Heinzel T, et al. A CBP integrator complex mediates transcriptional activation and AP-1 inhibition by nuclear receptors. *Cell.* 1996;85:403–14. [https://doi.org/10.1016/S0092-8674\(00\)81118-6](https://doi.org/10.1016/S0092-8674(00)81118-6).
- Keiter S, Grund S, van Bavel B, et al. Activities and identification of aryl hydrocarbon receptor agonists in sediments from the Danube river. *Anal Bioanal Chem.* 2008;390:2009–19. <https://doi.org/10.1007/s00216-007-1652-x>.
- Kleensang A. Pathways of toxicity. *ALTEX.* 2014;31:53–61. <https://doi.org/10.14573/altex.1309261>.
- Klinge CM, Kaur K, Swanson HI. The aryl hydrocarbon receptor interacts with estrogen receptor alpha and orphan receptors COUP-TFI and ERR α 1. *Arch Biochem Biophys.* 2000;373:163–74. <https://doi.org/10.1006/abbi.1999.1552>.
- Köhle C, Bock KW. Coordinate regulation of Phase I and II xenobiotic metabolisms by the Ah receptor and Nrf2. *Biochem Pharmacol.* 2007;73:1853–62. <https://doi.org/10.1016/j.bcp.2007.01.009>.
- Kushner PJ, Baxter JD, Duncan KG, et al. Eukaryotic regulatory elements lurking in plasmid DNA: the activator protein-1 site in pUC. *Mol Endocrinol.* 1994;8:405–7. <https://doi.org/10.1210/mend.8.4.8052261>.
- Leusch FDL, Snyder SA. Bioanalytical tools: half a century of application for potable reuse. *Environ Sci Water Res Technol.* 2015;1:606–21. <https://doi.org/10.1039/C5EW00115C>.
- Lillicrap A, Belanger S, Burden N, et al. Alternative approaches to vertebrate ecotoxicity tests in the 21st century: a review of developments over the last 2 decades and current status. *Environ Toxicol Chem.* 2016;35:2637–46. <https://doi.org/10.1002/etc.3603>.
- Lungu-Mitea S, Lundqvist J. Potentials and pitfalls of transient in vitro reporter bioassays: interference by vector geometry and cytotoxicity in recombinant zebrafish cell lines. *Arch Toxicol.* 2020. <https://doi.org/10.1007/s00204-020-02783-6>.
- Lungu-Mitea S, Oskarsson A, Lundqvist J. Development of an oxidative stress in vitro assay in zebrafish (*Danio rerio*) cell lines. *Sci Rep.* 2018;8:12380. <https://doi.org/10.1038/s41598-018-30880-1>.
- Lungu-Mitea S, Vogts C, Carlsson G, et al. Modeling bioavailable concentrations in zebrafish cell lines and embryos increases the correlation of toxicity potencies across test systems. *Environ Sci Technol.* 2021;55:447–57. <https://doi.org/10.1021/acs.est.0c04872>.
- Lushchak VI. Adaptive response to oxidative stress: bacteria, fungi, plants and animals. *Comp Biochem Physiol Part C Toxicol Pharmacol.* 2011;153:175–90. <https://doi.org/10.1016/j.cbpc.2010.10.004>.
- Ma Q, Kinneer K, Bi Y, et al. Induction of murine NAD(P)H:quinone oxidoreductase by 2,3,7,8-tetrachlorodibenzo-p-dioxin requires the CNC (cap “n” collar) basic leucine zipper transcription factor Nrf2 (nuclear factor erythroid 2-related factor 2): cross-interaction between AhR (aryl h. *Biochem J.* 2004;377:205–13. <https://doi.org/10.1042/BJ20031123>.
- Martino Mu, Alesci S, Gp C, Kino T. Interaction of the glucocorticoid receptor and the chicken ovalbumin upstream promoter-transcription factor II (COUP-TFII): implications for the actions of glucocorticoids on glucose, lipoprotein, and xenobiotic metabolism. *Ann N Y Acad Sci.* 2004;1024:72–85. <https://doi.org/10.1196/annals.1321.006>.
- Mattingly CJ, McLachlan JA, Toscano WA. Green fluorescent protein (GFP) as a marker of aryl hydrocarbon receptor (AhR) function in developing zebrafish (*Danio rerio*).

- Environ Health Perspect. 2001;109:845–9. <https://doi.org/10.2307/3454829>.
- Miao W, Hu L, Scrivens PJ, Batist G. Transcriptional regulation of NF-E2 p45-related factor (NRF2) expression by the aryl hydrocarbon receptor-xenobiotic response element signaling pathway. *J Biol Chem*. 2005;280:20340–8. <https://doi.org/10.1074/jbc.M412081200>.
- Miranda C, Collodi P, Zhao X, et al. Regulation of cytochrome P450 expression in a novel liver cell line from zebrafish (*Brachydanio rerio*). *Arch Biochem Biophys*. 1993;305:320–7. <https://doi.org/10.1006/abbi.1993.1429>.
- Mueller SO. Xenoestrogens: mechanisms of action and detection methods. *Anal Bioanal Chem*. 2004;378:582–7. <https://doi.org/10.1007/s00216-003-2238-x>.
- Mulholland DJ, Cox M, Read J, et al. Androgen responsiveness of Renilla luciferase reporter vectors is promoter, transgene, and cell line dependent. *Prostate*. 2004;59:115–9. <https://doi.org/10.1002/pros.20059>.
- Musset L. Current approaches in the statistical analysis of ecotoxicity data. OECD. 2018.
- Natesan S, Rivera VM, Molinari E, Gilman M. Transcriptional squelching re-examined. *Nature*. 1997;390:349–50. <https://doi.org/10.1038/37019>.
- Neale PA, Grimaldi M, Boulahtouf A, et al. Assessing species-specific differences for nuclear receptor activation for environmental water extracts. *Water Res*. 2020;185:116247. <https://doi.org/10.1016/j.watres.2020.116247>.
- Noury P, Geffard O, Tutundjian R, Garric J. Non destructive in vivo measurement of ethoxyresorufin biotransformation by zebrafish prolarva: Development and application. *Environ Toxicol*. 2006;21:324–31. <https://doi.org/10.1002/tox.20184>.
- NRC. Toxicity testing in the 21st Century. Washington, D.C.: National Academies Press; 2007.
- OECD. Test No. 236: Fish Embryo Acute Toxicity (FET) Test. OECD. 2013.
- Ohtake F, Takeyama K, Matsumoto T, et al. Modulation of oestrogen receptor signalling by association with the activated dioxin receptor. *Nature*. 2003;423:545–50. <https://doi.org/10.1038/nature01606>.
- Petrucci JR, Bunce NJ. Competitive inhibition by inducer as a confounding factor in the use of the ethoxyresorufin-O-deethylase (EROD) assay to estimate exposure to dioxin-like compounds. *Toxicol Lett*. 1999;105:251–60. [https://doi.org/10.1016/S0378-4274\(99\)00005-3](https://doi.org/10.1016/S0378-4274(99)00005-3).
- Raghunath A, Sundarraj K, Nagarajan R, et al. Antioxidant response elements: discovery, classes, regulation and potential applications. *Redox Biol*. 2018;17:297–314. <https://doi.org/10.1016/j.redox.2018.05.002>.
- Richter CA, Tieber VL, Denison MS, Giesy JP. An in vitro rainbow trout cell bioassay for aryl hydrocarbon receptor-mediated toxins. *Environ Toxicol Chem*. 1997;16:543–50. [https://doi.org/10.1897/1551-5028\(1997\)016%3c0543:AIVRTC%3e2.3.CO;2](https://doi.org/10.1897/1551-5028(1997)016%3c0543:AIVRTC%3e2.3.CO;2).
- Russell WMS, Burch RL. The principles of humane experimental technique. 1959.
- Safe S, Wang F, Porter W, et al. Ah receptor agonists as endocrine disruptors: antiestrogenic activity and mechanisms. *Toxicol Lett*. 1998;102–103:343–7. [https://doi.org/10.1016/S0378-4274\(98\)00331-2](https://doi.org/10.1016/S0378-4274(98)00331-2).
- Safe SH. Modulation of gene expression and endocrine response pathways by 2,3,7,8-tetrachlorodibenzo-p-dioxin and related compounds. *Pharmacol Ther*. 1995;67:247–81. [https://doi.org/10.1016/0163-7258\(95\)00017-B](https://doi.org/10.1016/0163-7258(95)00017-B).
- Sanderson JT, Aarts JMMJG, Brouwer A, et al. Comparison of Ah receptor-mediated luciferase and ethoxyresorufin-O-deethylase induction in H4IIE cells: implications for their use as bioanalytical tools for the detection of polyhalogenated aromatic hydrocarbons. *Toxicol Appl Pharmacol*. 1996;137:316–25. <https://doi.org/10.1006/taap.1996.0086>.
- Schlezinger JJ, Blickarz CE, Mann KK, et al. Identification of NF- κ B in the marine fish *Stenotomus chrysops* and examination of its activation by aryl hydrocarbon receptor agonists. *Chem Biol Interact*. 2000a;126:137–57. [https://doi.org/10.1016/S0009-2797\(00\)00161-7](https://doi.org/10.1016/S0009-2797(00)00161-7).
- Schlezinger JJ, Keller J, Verbrugge LA, Stegeman JJ. 3,3',4,4'-Tetrachlorobiphenyl oxidation in fish, bird and reptile species: relationship to cytochrome P450 1A inactivation and reactive oxygen production. *Comp Biochem Physiol C Toxicol Pharmacol*. 2000b;125:273–86. [https://doi.org/10.1016/S0742-8413\(99\)00112-7](https://doi.org/10.1016/S0742-8413(99)00112-7).
- Schlezinger JJ, Struntz WDJ, Goldstone JV, Stegeman JJ. Uncoupling of cytochrome P450 1A and stimulation of reactive oxygen species production by co-planar polychlorinated biphenyl congeners. *Aquat Toxicol*. 2006;77:422–32. <https://doi.org/10.1016/j.aquatox.2006.01.012>.
- Schlezinger JJ, White RD, Stegeman JJ. Oxidative inactivation of cytochrome P-450 1A (CYP1A) stimulated by 3,3',4,4'-tetrachlorobiphenyl: production of reactive oxygen by vertebrate CYP1As. *Mol Pharmacol*. 1999;56:588–97. <https://doi.org/10.1124/mol.56.3.588>.
- Schmidt JV, Bradfield CA. AH receptor signaling pathways. *Annu Rev Cell Dev Biol*. 1996;12:55–89. <https://doi.org/10.1146/annurev.cellbio.12.1.55>.
- Shifera AS, Hardin JA. Factors modulating expression of Renilla luciferase from control plasmids used in luciferase reporter gene assays. *Anal Biochem*. 2010;396:167–72. <https://doi.org/10.1016/j.ab.2009.09.043>.
- Shifera AS, Hardin JA. PMA induces expression from the herpes simplex virus thymidine kinase promoter via the activation of JNK and ERK in the presence of adenoviral E1A proteins. *Arch Biochem Biophys*. 2009;490:145–57. <https://doi.org/10.1016/j.abb.2009.08.013>.
- Shin S, Wakabayashi N, Misra V, et al. NRF2 modulates aryl hydrocarbon receptor signaling: influence on adipogenesis. *Mol Cell Biol*. 2007;27:7188–97. <https://doi.org/10.1128/MCB.00915-07>.
- Simmons SO, Fan C-Y, Ramabhadran R. Cellular stress response pathway system as a sentinel ensemble in toxicological screening. *Toxicol Sci*. 2009;111:202–25. <https://doi.org/10.1093/toxsci/kfp140>.
- Simon TW, Budinsky RA, Rowlands JC. A model for aryl hydrocarbon receptor-activated gene expression shows potency and efficacy changes and predicts squelching due to competition for transcription co-activators. *PLoS ONE*. 2015;10:e0127952. <https://doi.org/10.1371/journal.pone.0127952>.

- Soshilov AA, Denison MS. Ligand promiscuity of aryl hydrocarbon receptor agonists and antagonists revealed by site-directed mutagenesis. *Mol Cell Biol*. 2014;34:1707–19. <https://doi.org/10.1128/MCB.01183-13>.
- Stepanenko AA, Heng HH. Transient and stable vector transfection: pitfalls, off-target effects, artifacts. *Mutat Res Rev Mutat Res*. 2017;773:91–103. <https://doi.org/10.1016/j.mrrev.2017.05.002>.
- Swanson HI, Chan WK, Bradfield CA. DNA binding specificities and pairing rules of the Ah receptor, ARNT, and SIM proteins. *J Biol Chem*. 1995;270:26292–302. <https://doi.org/10.1074/jbc.270.44.26292>.
- Tanguay RL, Abnet CC, Heideman W, Peterson RE. Cloning and characterization of the zebrafish (*Danio rerio*) aryl hydrocarbon receptor. *Biochim Biophys Acta - Gene Struct Expr*. 1999;1444:35–48. [https://doi.org/10.1016/S0167-4781\(98\)00252-8](https://doi.org/10.1016/S0167-4781(98)00252-8).
- Tanguay RL, Andreassen E, Heideman W, Peterson RE. Identification and expression of alternatively spliced aryl hydrocarbon nuclear translocator 2 (ARNT2) cDNAs from zebrafish with distinct functions. *Biochim Biophys Acta - Gene Struct Expr*. 2000;1494:117–28. [https://doi.org/10.1016/S0167-4781\(00\)00225-6](https://doi.org/10.1016/S0167-4781(00)00225-6).
- Terenzi F, DeVeer MJ, Ying H, et al. The antiviral enzymes PKR and RNase L suppress gene expression from viral and non-viral based vectors. *Nucleic Acids Res*. 1999;27:4369–75. <https://doi.org/10.1093/nar/27.22.4369>.
- The European Parliament and of the Council. Regulation (EC) No 1831/2003 of the European Parliament and of the Council of 22 September 2003 on additives for use in animal nutrition. 2003.
- The European Parliament and of the Council. Regulation (EC) No 1907/2006 concerning the Registration, Evaluation, Authorization and Restriction of Chemicals (REACH). 2006.
- The European Parliament and of the Council. Regulation (EC) No 1107/2009 of the European Parliament and of the Council of 21 October 2009 concerning the placing of plant protection products on the market and repealing Council Directives 79/117/EEC and 91/414/EEC. 2009.
- Tian Y. Ah receptor and NF- κ B interplay on the stage of epigenome. *Biochem Pharmacol*. 2009;77:670–80. <https://doi.org/10.1016/j.bcp.2008.10.023>.
- Tysklind M, Bosvelt TCA, Andersson P, et al. Induction of erod activity in european Eel (*Anguilla anguilla*) by different polychlorobiphenyls (PCBs). *Water Sci Technol*. 1998;38:211–6. [https://doi.org/10.1016/S0273-1223\(98\)00625-8](https://doi.org/10.1016/S0273-1223(98)00625-8).
- Ulin A, Henderson J, Pham M-T, et al. Developmental regulation of nuclear factor erythroid-2 related factors (nrfs) by AHR1b in zebrafish (*Danio rerio*). *Toxicol Sci*. 2019;167:536–45. <https://doi.org/10.1093/toxsci/kfy257>.
- US EPA. The Frank R. Lautenberg Chemical Safety for the 21st Century Act: Frequent Questions. 2016;1–67.
- Verhallen EY, van den Berg M, Bosveld ATC. Interactive effects on the erod-inducing potency of polyhalogenated aromatic hydrocarbons in the chicken embryo hepatocyte assay. *Environ Toxicol Chem*. 1997;16:277–82. <https://doi.org/10.1002/etc.5620160225>.
- Villeneuve DL, Richter CA, Blankenship AL, Giesy JP. Rainbow trout cell bioassay-derived relative potencies for halogenated aromatic hydrocarbons: comparison and sensitivity analysis. *Environ Toxicol Chem*. 1999;18:879–88. <https://doi.org/10.1002/etc.5620180510>.
- Wang X, Xu Z, Tian Z, et al. The EF-1 α promoter maintains high-level transgene expression from episomal vectors in transfected CHO-K1 cells. *J Cell Mol Med*. 2017;21:3044–54. <https://doi.org/10.1111/jcmm.13216>.
- Wassenberg DM, Nerlinger AL, Battle LP, Di GRT. Effects of the polycyclic aromatic hydrocarbon heterocycles, carbazole and dibenzothiophene, on in vivo and in vitro cyp1a activity and polycyclic aromatic hydrocarbon-derived embryonic deformities. *Environ Toxicol Chem*. 2005;24:2526. <https://doi.org/10.1897/04-440R1.1>.
- Weimer M, Jiang X, Ponta O, et al. The impact of data transformations on concentration–response modeling. *Toxicol Lett*. 2012;213:292–8. <https://doi.org/10.1016/j.toxlet.2012.07.012>.
- Wernersson A-S, Carere M, Maggi C, et al. The European technical report on aquatic effect-based monitoring tools under the water framework directive. *Environ Sci Eur*. 2015;27:7. <https://doi.org/10.1186/s12302-015-0039-4>.
- Whelan M, Andersen M. Toxicity pathways — from concepts to application in chemical safety assessment (EUR 26389 EN). 2013.
- White RD, Shea D, Coloww AR, Stegeman JJ. Induction and post-transcriptional suppression of hepatic cytochrome p450 1a1 by 3,3',4,4'-tetrachlorobiphenyl. *Biochem Pharmacol*. 1997;53:1029–40. [https://doi.org/10.1016/S0006-2952\(96\)00902-1](https://doi.org/10.1016/S0006-2952(96)00902-1).
- Worth A, Barroso J, Bremer S, et al. Alternative methods for regulatory toxicology — a state-of-the-art review. 2014.
- Wright EJ, Pereira De Castro K, Joshi AD, Elferink CJ. Canonical and non-canonical aryl hydrocarbon receptor signaling pathways. *Curr Opin Toxicol*. 2017;2:87–92. <https://doi.org/10.1016/j.cotox.2017.01.001>.
- Xu C, Pasco DS. Suppression of CYP1A1 transcription by H2O2Is mediated by xenobiotic-response element. *Arch Biochem Biophys*. 1998;356:142–50. <https://doi.org/10.1006/abbi.1998.0770>.
- Yang J, Zhu J, Chan KM. BDE-99, but not BDE-47, is a transient aryl hydrocarbon receptor agonist in zebrafish liver cells. *Toxicol Appl Pharmacol*. 2016;305:203–15. <https://doi.org/10.1016/j.taap.2016.06.023>.
- Yeager RL, Reisman SA, Aleksunes LM, Klaassen CD. Introducing the “TCDD-Inducible AhR-Nrf2 Gene Battery.” *Toxicol Sci*. 2009;111:238–46. <https://doi.org/10.1093/toxsci/kfp115>.
- Zacharewski T. In vitro bioassays for assessing estrogenic substances. *Environ Sci Technol*. 1997;31:613–23. <https://doi.org/10.1021/es960530o>.
- Zeruth G, Pollenz RS. Isolation and characterization of a dioxin-inducible CYP1A1 promoter/enhancer region

- from zebrafish (*Danio rerio*). *Zebrafish*. 2005;2:197–210. <https://doi.org/10.1089/zeb.2005.2.197>.
- ZeRuth G, Pollenz RS. Functional analysis of cis-regulatory regions within the dioxin-inducible CYP1A promoter/enhancer region from zebrafish (*Danio rerio*). *Chem Biol Interact*. 2007;170:100–13. <https://doi.org/10.1016/j.cbi.2007.07.003>.
- Zhao H, Li H, Du J, et al. Regulation of ddb2 expression in blind cavefish and zebrafish reveals plasticity in the control of sunlight-induced DNA damage repair. *PLOS Genet*. 2021;17:e1009356. <https://doi.org/10.1371/journal.pgen.1009356>.
- Zhou Z, Yang J, Chan KM. Toxic effects of triclosan on a zebrafish (*Danio rerio*) liver cell line, ZFL. *Aquat Toxicol*. 2017;191:175–88. <https://doi.org/10.1016/j.aquatox.2017.08.009>.

Publisher's note Springer Nature remains neutral with regard to jurisdictional claims in published maps and institutional affiliations.